Seasonal and regional signatures of ENSO in upper tropospheric jet characteristics from reanalyses

Gloria L Manney*

NorthWest Research Associates & New Mexico Institute of Mining and Technology, Socorro, New Mexico, USA

Michaela I Hegglin

Department of Meteorology, University of Reading, Reading, UK.

Zachary D Lawrence†

Cooperative Institute for Research in Environmental Sciences (CIRES) & NOAA Physical Sciences Laboratory (PSL), University of Colorado, Boulder, Colorado, USA.

Corresponding author address: Dept. of Physics, New Mexico Institute of Mining and Technology, Socorro, New Mexico, 87801, USA.

E-mail: manney@nwra.com

†Also at NorthWest Research Associates, Boulder, CO, USA.

ABSTRACT

Regionally and seasonally resolved relationships of upper tropospheric jet variability to El Niño / Southern Oscillation (ENSO) in multiple reanalyses are presented, with subtropical and polar jets analyzed separately. Previously reported results confirmed herein include strengthening of tropical jets associated with monsoons and Walker circulation during La Niña and a statistically significant subtropical jet latitude decrease (increase) during El Niño (La Niña) in the zonal mean view in both hemispheres. However, subtropical jet latitudes increase significantly during El Niño over the NH eastern Pacific in DJF, and in different limited SH regions in MAM and SON. Subtropical jet altitudes increase significantly during El Niño in the zonal mean in all seasons (DJF / MAM) in the NH (SH). Subtropical jet windspeed correlations with ENSO vary, showing increasing windspeed during El Niño in both hemispheres in DJF and MAM. Polar jet correlations with ENSO are typically not significant in the zonal mean, but there are a few regions/seasons with significant correlations with ENSO, particularly in the SH, where polar jet latitudes decrease over Asia and the western Pacific in DJF, and increase over the eastern Pacific in JJA and SON, during El Niño. Typically, significantly weaker (stronger) polar jet windspeeds are associated with El Niño (La Niña) in the western than in the eastern hemisphere in both NH and SH. All reanalyses analyzed agree well. This work highlights the importance of regional and seasonal variations in the upper tropospheric jet response to ENSO and provides new information for model evaluation.

1. Introduction

Jet streams in the upper troposphere (UT) are a crucial are a prominent feature of the atmospheric circulation and play an essential role in variability in phenomena such as storm tracks, precipitation, and extreme weather events (Uccellini and Johnson 1979; Nakamura et al. 2004; Kolstad et al. 2010; Grotjahn et al. 2016; Harnik et al. 2016; Mann et al. 2017; Winters et al. 2019, and references therein). UT jets are sensitive to climate change and ozone loss, as well as to natural modes of variability (Lorenz and DeWeaver 2007; Scaife et al. 2008; McLandress et al. 2011; Hudson 2012; Lin et al. 2014, 2015; Waugh et al. 2015, 2018; Grise et al. 2018, and references therein). They are instrumental in determining upper troposphere / lower stratosphere (UTLS) composition and its changes (Manney et al. 2011; Minschwaner et al. 2015; Olsen et al. 2016, 2019; Díaz and Vera 2017, and references therein).

While the extratropical UT jets are commonly (and usefully) classified as radiatively driven (the "subtropical" jet) or eddy driven (the "polar" jet) (e.g., Held and Phillips 1990), their observed structure shows a complex seasonally and regionally varying spectrum from which separate radiatively and eddy-driven jets cannot easily be identified (e.g, Manney et al. 2014; Manney and Hegglin 2018). This view is consistent with the complex interplay of dynamical and radiative processes on multiple scales, as well as landmass and orography distributions (e.g., Hoskins and Valdes 1990; Held et al. 2002; Lee and Kim 2003), that determine their structure and evolution. Because of the complexity of the processes shaping the upper tropospheric circulation and thus the structure and evolution of the jets, it is difficult to predict or model their responses to climate change and to disentangle that response from that to natural modes of variability (e.g., Garfinkel et al. 2015; Lucas and Nguyen 2015; Waugh et al. 2015; Grise et al. 2019). This difficult task is important because changes in UT jet streams are linked to changing regional weather and climate

patterns (Lucas et al. 2014; Harnik et al. 2016; Mann et al. 2017; Winters et al. 2019, and references therein). Both tropical and extratropical UT jets have been linked to rainfall changes in the tropics (e.g., Hulme and Tosdevin 1989; Bollasina et al. 2014; Kelly et al. 2018; RavindraBabu et al. 2019), subtropics (e.g., Price et al. 1998; Raible et al. 2004; Lucas et al. 2014; Huang et al. 2015; Xie et al. 2015), and midlatitudes (e.g., Kang et al. 2011; Thompson et al. 2011; Delworth and Zeng 2014; Bai et al. 2016; Zhao et al. 2018), which are also often correlated to changes in sea surface temperatures (SSTs) such as those during El Niño / Southern Oscillation (ENSO) events. It is also critical because of the jets' importance to UTLS composition and stratosphere-troposphere exchange (STE), which have also been shown to have relationships to ENSO (e.g., Zeng and Pyle 2005; Oman et al. 2011; Lin et al. 2014, 2015; Olsen et al. 2016, 2019).

Many studies, both modeling and observational suggest widening of the tropics resulting from climate change and a concomitant poleward shift of the subtropical UT jets, though with very large uncertainties in their magnitude (Lorenz and DeWeaver 2007; Strong and Davis 2007, 2008; Lucas et al. 2014; Staten et al. 2016; Maher et al. 2019, and references therein). Until recently most studies were of zonal means or averages in broad regions, but a few studies suggested narrowing rather than widening of the tropics in specific regions and seasons (e.g., Lucas et al. 2012; Peña-Ortiz et al. 2013; Lucas and Nguyen 2015). Manney and Hegglin (2018) conducted a detailed study of regional and seasonal variability in UT jets that confirms regionally confined tropical widening only across Africa (except during NH spring), extending into Asia and the western Pacific during NH summer. In contrast, the study shows regions of tropical narrowing during NH winter from the central Pacific across North America and the western Atlantic; they thus found only few regions / seasons with robust trends in the subtropical UT jets in reanalyses. There has also been considerable controversy about climate related changes in the polar UT jets and their relationships to Arctic amplification and the "waviness" of the jets (Barnes and Screen 2015; Overland et al. 2016;

Shepherd 2016; Francis 2017, and references therein); Manney and Hegglin (2018) showed, as for the subtropical jets, large regional and seasonal variability in trends in polar UT jets, but indicated many regions / seasons with robust equatorward shifts of those jets, especially in the NH (except over North America), suggesting a wave-like longitudinal pattern in the jet response to climate change that would support the notion of the jets becoming wavier or more variable.

ENSO is a climate phenomenon that describes oscillating SSTs and associated atmospheric wind patterns over the tropical ocean in the central and eastern Pacific, which influences weather and precipitation across the globe (e.g., Rasmusson and Carpenter 1982; Wolter and Timlin 2011; Zhang et al. 2019, and references therein). El Niño refers to the warm phase and La Niña to the cold phase of the oscillation. ENSO is one of the natural modes of variability that have been shown to influence the upper tropospheric and stratospheric circulation (see, e.g., Domeisen et al. 2019, for a review) (e.g., Yulaeva and Wallace 1994; Shapiro et al. 2001; Calvo et al. 2010, and references therein). While some studies focus on relationships to zonal mean winds and temperatures (e.g., Yulaeva and Wallace 1994; Randel et al. 2009; Calvo et al. 2010, and references therein), regional circulation impacts of ENSO affecting the UTLS have also long been recognized (e.g., Shapiro et al. 2001, and reference therein). Numerous studies have linked variations in metrics of Asian summer monsoon (ASM) intensity and timing to ENSO conditions (see review in Bombardi et al. 2020), including several that examine upper tropospheric circulation diagnostics (e.g., Tweedy et al. 2018; Yan et al. 2018), which are in turn closely related to UT jet changes associated with the ASM circulation (Schiemann et al. 2009; Manney et al. 2014, 2020, and references therein), though there is no consensus because of the variety and complexity of relationships and diagnostics used. In addition, several studies have shown regional changes in UT jets (and their implications for transport) that are related to ENSO (e.g., Langford 1999; Lucas and Nguyen 2015; Lin et al. 2014, 2015; Olsen et al. 2016, 2019). To our knowledge, no comprehensive study has quantified

the relationships of ENSO to the UT jets (tropical, subtropical, and polar) over the full range of regional and seasonal variability.

The JEt and Tropopause Products for Analysis and Characterization (JETPAC) software and products, developed by Manney et al. (2011) and Manney and Hegglin (2018), has been used (among several other studies) to provide a comprehensive climatology of UT jets (Manney et al. 2014), for detailed reanalysis comparisons of UT jets (Manney et al. 2017), and by Manney and Hegglin (2018) in a comprehensive study of regional and seasonal patterns of trends in reanalyses. Because characteristics identified by analysis of patterns, such as jet core locations and dynamical variables at those locations, are not amenable to direct observation, reanalyses from modern data assimilation systems are our primary tools for studying such phenomena. Numerous recent studies, particularly related to the Stratosphere-troposphere Processes and their Role in Climate (SPARC)-Reanalysis Intercomparison project (S-RIP) (Fujiwara et al. 2017), highlight the importance of comparing results among reanalyses – e.g., in the S-RIP final report (in press), see Chapters 7 (The Extra-tropical UTLS) (Homeyer et al. 2020) and 8 (The Tropical Tropopause Layer, which includes a section on tropical width) (Tegtmeier et al. 2020b); also see related papers in the S-RIP ACP / ESSD Special Issue that are relevant to UTLS dynamics (e.g. Martineau et al. 2018; Diallo et al. 2019; Xian and Homeyer 2019; Tegtmeier et al. 2020a; Wright et al. 2020). Manney and Hegglin (2018) found it was critical to evaluate multiple reanalyses to help determine the robustness of trends in the UTLS jet streams.

In this paper, we use JETPAC products updated from Manney and Hegglin (2018) to study the relationships of UT jets to ENSO in reanalyses from 1979 through 2018. Our results provide a comprehensive view of these relationships broken down by region and season, and are presented for multiple reanalyses. Section 2 describes the datasets and methods used; Section 3a compares

geographic patterns for El Niño and La Niña periods; Section 3b discussed correlations between ENSO and jet characteristics by region and season. Our conclusions are given in Section 4.

2. Data and Methods

a. Reanalysis Datasets

We use JETPAC (Manney et al. 2011, see below, Section 2b1) to calculate jet core latitude, altitude, and windspeed for polar and subtropical UT jets from three modern "full-input" reanalyses: NASA's Global Modeling and Assimilation Office's Modern Era Retrospective-analysis for Research and Applications, version-2 (MERRA-2) reanalysis (Gelaro et al. 2017); ECMWF's ERA-Interim reanalysis Dee et al. (2011a); and the JMA's 55-year (JRA-55) reanalysis (Ebita et al. 2011; Kobayashi et al. 2015). We focus on the aforementioned three reanalyses based on previous intercomparison studies; not shown are analysis of MERRA and NCEP's CFSR/CFSv2 (Climate Forecast System Reanalysis / Climate Forecast System Version 2; this reanalysis has been shown to have issues with discontinuities and poorer agreement with data and other modern reanalyses for many diagnostics in the UTLS, e.g., Long et al. 2017; Manney et al. 2017; Xian and Homeyer 2019; Homeyer et al. 2020). CFSR/CFSv2 on model levels and MERRA are also only available through 2015, but we have conducted the calculations described herein with these two reanalyses for 1979 through 2015, and the results are generally consistent with the three reanalyses shown.

Table 1 summarizes the information about the reanalyses products studied herein that is most relevant to this paper. One feature of MERRA Rienecker et al. (2011) and MERRA-2 (Gelaro et al. 2017) that is different from the other reanalyses is that the assimilation system uses an Incremental Analysis Update (IAU) (Bloom et al. 1996) to constrain the analyses. Both "Analyzed"

(prior to IAU) and "Assimilated" (after IAU) data collections are provided by GMAO; we use here the Assimilated data collection (Global Modeling and Assimilation Office (GMAO) 2015), as recommended by GMAO for most studies (see, e.g., https://gmao.gsfc.nasa.gov/reanalysis/MERRA-2/docs/ANAvsASM.pdf and Fujiwara et al. 2017); differences between ANA and ASM are usually small, but not always negligible (e.g., Manney et al. 2017). 1979 is considered a spin-up year for MERRA-2, and thus those data are not in the public record; we use data for December 1979 here in the seasonal calculations for DJF. The models, assimilation systems, and data inputs for the reanalyses are described in detail by Fujiwara et al. (2017).

Calculations are done using daily 12-UT fields from each reanalysis dataset, and the reanalysis fields are used on their native model levels and at or (in the case of spectral models) near the native horizontal resolution, as indicated in Table 1. The vertical resolution in the UTLS (which has been shown to be critical for representation of UT jets and tropopauses, e.g., Manney et al. 2017) for each of these reanalyses is near 1 km, depending on the exact level, slightly lower for CFSR/CFSv2 and slightly higher for MERRA and MERRA-2 (see Table 1 and Fujiwara et al. 2017, their Figure 3).

b. Methods

1) JETPAC

Upper tropospheric jet characteristics are calculated using JETPAC (Manney et al. 2011, 2014, 2017; Manney and Hegglin 2018). Jet core location frequency distributions are calculated in 3° latitude by 6° longitude bins, and normalized by the number of jets that would "fill" each bin if one were identified at every longitude in that bin; results are expressed in percent. Because the JRA-55 Gaussian grid on which that dataset is provided does not have an integer number of gridpoints in each bin, the JRA-55 data are interpolated to a $0.5^\circ \times 0.5^\circ$ latitude $\times$ longitude grid

before computing frequency distributions (the native grid is used for the other analyses in this paper). (See Manney et al. 2014, 2017, for further details on binning and normalization).

The subtropical jet is identified (as described by Manney and Hegglin 2018) as the jet across which the "tropopause break" occurs. The polar jet is taken to be the strongest westerly jet poleward of the subtropical jet (or poleward of 40° latitude if there is no subtropical jet); as was the case in Manney and Hegglin (2018), the results are insensitive to the details of the polar jet definition once the subtropical jet is accounted for. These criteria provide physically meaningful definitions that distinguish the jets that most closely approximate the idealized "radiatively-driven" (the subtropical jet) and "eddy-driven" (the polar jet) types.

2) Analysis

Relationships with ENSO are assessed using composites for extremes of and correlations with the Multivariate ENSO Index version 2 (MEIv2) (Zhang et al. 2019), which is an adaptation of the widely used MEI described by Wolter and Timlin (2011). The calculations in this paper were also done using the MEI, with very similar results.

Supplementary Figures S1–S4 show results of tests of sensitivity to the threshold MEIv2 magnitudes for El Niño or La Niña conditions, as well as to comparing El Niño to La Niña composites versus comparing each to neutral conditions. The comparisons with climatology and neutral states (Figures S1 and S2 show SON; results for other seasons are similar) demonstrate that the anomalies from those states in each case are qualitatively very similar to those for the El Niño / La Niña anomalies, but less intense; we thus show anomalies as La Niña − El Niño hereinafter. Similarly, we checked thresholds of 0.94, 0.7, and 0.56 for MEIv2 magnitude; Figures S3 and S4 show that all three choices give very similar results, and we show composites using 0.94 hereinafter. (Com-

paring Figures S1 and S2 with S3 and S4 also shows that choosing different neutral thresholds does not qualitatively change comparisons of ENSO periods with neutral composites.)

For the correlations, as in Manney and Hegglin (2018), the latitude, altitude, and windspeed of the subtropical and polar jets were calculated at each longitude of the reanalysis grids for each day using 1200UTC fields; these are averaged by month and season (DJF, MAM, JJA, and SON), zonally and in 20° longitude bins (from 180–160°W through 160–180°E). The 40-year record (from 1979 through 2018, except 1979/1980 through 2018/2019 for DJF) for these periods and longitude regions is then correlated with the MEIv2 index time series for the corresponding month or season. Both MEIv2 and jet diagnostic time series are detrended before the correlations are calculated. Using the methods of Manney and Hegglin (2018) to identify linear trends, the MEIv2 index shows negative trends (that is, towards more La Niña conditions) in all seasons over 1979–2018 with confidence levels of 79, 91, 83, and 74% in DJF, MAM, JJA, and SON, respectively.

Figure 1 provides a schematic of the physical changes associated with negative or positive correlations between the upper tropospheric jet characteristics and ENSO. Thus, if the correlation is positive (following the bold arrows) if ENSO is in the El Niño phase the latitude, altitude, or windspeed would increase, with the opposite changes in the La Niña phase. Conversely, for a negative correlation, latitude, altitude, and windspeed would increase during La Niña and decrease during El Niño. There is no expectation that the signs of correlations between ENSO and each of the variables (jet latitude, altitude, and windspeed) will be the same for a given region and season, and indeed we show below that they generally are not.

The statistical significance of the correlations is assessed using simple bootstrap resampling (e.g., Elfron and Tibshirani 1993) to construct 100,000 artificial time series based on the input data time series. This was used to construct 95 and 99% confidence intervals for the correlations. Since our time series comprising means for a given month or season over a number of years are

not expected to have much autocorrelation/sample dependence, and are only 40 years long, there is no reason to expect using a block bootstrapping method is necessary, though we have also done the calculations using fixed block and "stationary" (Politis and Romano 1994) bootstrapping with results very similar to those shown here. (See, e.g., Lawrence et al. 2018; Lawrence and Manney 2020, for further details of bootstrapping methods.)

3. Results

a. Jet Distributions by ENSO Phase

Figure 2 shows composite maps of jet core frequency distributions for El Niño and La Niña conditions and the differences between them for the MERRA-2 reanalysis; Fig. 3 shows similar distributions in the latitude / altitude plane. (Note that the anomalies are the absolute (as opposed to percent) differences between two fields that were expressed in percent.) Supplementary Figs. S5 through S8 show the corresponding distributions for ERA-Interim and JRA-55; differences between the reanalyses appear to be small and quantitative rather than qualitative.

The differences between El Niño and La Niña distributions vary strongly with region, but in general show that subtropical jets are further poleward during La Niña than El Niño periods. This result suggests relationships of ENSO to the subtropical UT jets may show similar features to the relationships of ENSO to surface westerlies (e.g., Chen et al. 2008). This pattern is clear in regions where the subtropical jet is strong and relatively zonal, except in the NH in DJF over Africa and Asia, where the differences are less strong and could suggest a slightly weaker subtropical jet during La Niña periods (that is, the anomalies show a tripole pattern with negative values along the jet core, rather than a dipole pattern that would clearly indicate a jet shift). The anomalies are in general weaker in DJF in both hemispheres, strong in the SH in all other seasons, and strongest in

the NH during MAM. A poleward subtropical jet shift for La Niña conditions in the Asian Summer Monsoon (ASM) region in JJA is consistent with the results of Manney et al. (2020) showing a positive correlation between subtropical jet latitude and ASM anticyclone centroid latitude, and a negative correlation of ASM anticyclone centroid latitude with MEI.

Patterns with respect to higher latitude jets are more difficult to interpret: The patterns in the south Pacific (from about 130°E through 180°W to 45°W) suggest an equatorward shift of the polar jet during La Niña. A similar, but weaker, pattern is suggested in MAM and SON over North America, the Atlantic, and Asia, and in SON over the western north Pacific, but the complexity of the jet distributions in these regions (e.g., see Manney et al. 2014) preclude precise attribution of the origins of these patterns. In the SH, especially in JJA and SON, the anomalies in the region where the climatological subtropical jet spirals in to join the polar jet (between ∼90°W and 45°E, e.g., Williams et al. 2007; Manney et al. 2014) are consistent with an equatorward shift of that "transitional" jet during La Niña conditions (though only weakly in DJF).

Strengthening of the tropical easterly jet associated with the Asian Summer Monsoon (ASM) anticyclone during La Niña is apparent in JJA and SON. This is consistent with previous work suggesting stronger monsoons during La Niña conditions, though many of those studies assess rainfall or other surface characteristics that are indirectly related to the UT circulation (Ju and Slingo 1995; Zhang et al. 1999; Li et al. 2017; Tweedy et al. 2018; Bombardi et al. 2020, and references therein) The tropical westerly jet just south of the equator in SON, DJF, and JJA (near 140°W to 90°W, Manney et al. 2014) is associated with the Walker circulation with upper-level westerlies downstream of the upper level easterlies associated with the Australian monsoon. This is also consistent with previous work showing a stronger Walker circulation during La Niña periods (e.g., Julian and Chervin 1978; Tanaka et al. 2004b; Bayr et al. 2014); Manney and Hegglin (2018) noted that strengthening of the tropical westerly jet associated with the Walker circulation over

1979–2015 in DJF was consistent with a dominance of La Niña over El Niño conditions in DJF in the late part of that time period, and vice versa in the early part, indicating that some UT jet trends in that season are linked to ENSO trends.

Figure 3 shows a zonal mean view of the jet frequency distributions in the latitude / altitude plane. The poleward shift of the subtropical jet during La Niña seen in several regions in Fig. 2 is apparent in the SH in JJA and SON, where it is accompanied by a slight downward shift in altitude. This pattern is apparent in all seasons in the NH, though weakly in DJF and JJA. In the latter period, this is likely because the subtropical jet latitude varies strongly regionally as it shifts northward around the ASM circulation (e.g. Schiemann et al. 2009; Manney et al. 2014), and thus the zonally averaged frequency distributions do not capture the regional character of that jet. In MAM and JJA, the downward shift accompanying the poleward one is stronger than in the SH. In MAM, all of the extratropical jets show a downward shift during La Niña periods. Because the NH jets are even less well-characterized by the sub-tropical jet / polar jet taxonomy, and have even stronger regional and seasonal variations (e.g., Manney et al. 2014), these associations cannot capture the full range of variations with ENSO conditions.

The tropical jets (easterly versus westerly not being distinguished in this view) all clearly show strengthening during La Niña conditions, consistent with previous work relating ENSO variations to tropical circulations and jets (e.g., Tanaka et al. 2004a; Shaman and Tziperman 2007; Bayr et al. 2014); there is no evidence of an altitude shift in the tropical jets in the zonal mean.

The above qualitative picture shows strong variations by both region and season in the relationships of UT jet characteristics to ENSO conditions. To quantify these relationships of the UT jets to ENSO, in the next section we examine correlations of the MEIv2 index with subtropical and polar jet latitude, altitude, and windspeed, as a function of region and season.

b. Jet / ENSO Correlations

Figures 4 and 5 show correlations of jet latitude (absolute value in the SH), altitude, and windspeed with MEIv2 for the three reanalyses in the zonal mean as a function of month and season.

The subtropical jet (Fig. 4) shows significant negative latitude and positive altitude correlations with MEIv2 in most months and seasons, and both hemispheres, indicating a robust poleward and downward shift of the subtropical jet during La Niña periods. In all cases, the signs of the correlations agree among the reanalyses, and the magnitudes are typically quite similar, with no obvious pattern of which reanalysis shows strongest correlations. Seasonal latitude correlations in the NH are significant in all cases except for MERRA-2 in DJF; in the SH, seasonal correlations are significant except for MERRA-2 in MAM. Seasonal altitude correlations are significant in all seasons and reanalyses in the NH, and in DJF and MAM in the SH, consistent with the broad altitude decreases seen in Fig. 3. These seasonal results are based on significant correlations in most months in the NH (Dec, Jan, Mar, Apr latitude correlations are not significant, and Jan, Jun, Jul altitude correlations are not significant), and significant latitude correlations in Jan–Apr and Sep, and altitude correlations in Jan–May and (except for ERA-Interim) Nov–Dec in the SH. The monthly correlations that are not significant are negative for latitude except in Jun in the SH, and always positive for altitude.

Subtropical jet windspeed correlations are less consistent, but significant positive correlations (indicating weaker windspeeds during La Niña) are seen in the NH in Jan–Apr, DJF, and MAM; Oct and SON show significant negative windspeed correlations (stronger windspeeds during La Niña) in the NH. In the SH, the windspeed correlations are always positive and are significant in Jun, Oct–Nov, MAM, and SON.

Correlations of MEIv2 with polar jet characteristics (Fig. 5) are much less consistent / significant than those with the subtropical jet, possibly because of the complexity of / indirect effects associated with tropical-extratropical teleconnections affecting these relationships (e.g., Stan et al. 2017). Significant negative latitude correlations (i.e., poleward shift during La Niña) are seen in the NH for some reanalyses in Apr, Jul,and JJA, and in the SH in Dec and DJF. The latter result is similar to the findings of Byrne et al. (2017, 2019) for the SH lower tropospheric eddy-driven jet – they found that ENSO affects that jet primarily via the stratospheric polar vortex, and only during December. Significant positive altitude correlations (i.e., downward shift during La Niña) are seen in the NH in Apr and MAM, and in the SH in Jan–Mar, DJF, and MAM, and in MERRA-2 only in Apr-Jun and Nov. In the NH, significant negative windspeed correlations (i.e., stronger windspeeds during La Niña) are seen in Jan, Mar, and DJF; in the SH, significant positive windspeed correlations are seen in Aug, and significant negative correlations in Nov–Dec and DJF.

Because of strong regional variability (as seen in Fig. 2), regionally resolved correlations provide more insight into these relationships. Figures 6 through 13 show correlations in 20° longitude regions in each season for subtropical and polar jets.

Figure 6 shows that for DJF, the negative correlations of MEIv2 with subtropical jet latitude (i.e., poleward shift during La Niña) are limited to 120–80°W and 20–140°E in the NH, and 140°E–140°W, 100–60°W, and 20°W–0° in the SH. Significant positive latitude correlations are seen in the eastern Pacific (160–140°W) in the NH, and in MERRA-2 and JRA-55 near 20–40°E in the SH. These variations in the latitude correlations seem consistent with the smaller and not always significant latitude correlations seen in the zonal mean during this season (Fig. 4). Significant altitude correlations are always positive in both hemispheres (i.e., downward shifts in altitude during La Niña), and are seen from 140–80°W and 20°W–120°E in all regions except 0–140°E in the SH. In the NH, significant positive windspeed correlations (i.e., weakening windspeeds during

La Niña) are seen at 180–40°W and significant negative correlations at 100-140°E. Windspeed correlations in the SH are significantly negative at 160–80°W and 120–140°E, and significantly positive from 60°W through 100°E.

In MAM (Fig. 7), there are significant negative subtropical jet latitude correlations (i.e., a poleward shifts during La Niña) in the NH from 120–80°W and 60–120°E, and in the SH from 180–60°W and in MERRA-2 and JRA-55 at 60–80°E; significant positive latitude correlations (i.e., an equatorward shifts during La Niña) are seen in the SH at 40°W through 20°E. All significant altitude correlations are positive (i.e., downward shifts in altitude during La Niña) and in the NH cover all regions except near the Greenwich meridian and about 40° east and west of the dateline; significant positive altitude correlations in the SH are from 160°E across the dateline through 40°W and 60–100°E. Positive windspeed correlations (i.e., weakening of windspeeds during La Niña) in the NH are seen at 160–60°W and 20–60°E, with negative correlations at 40°W–0° and 100–140°E. In the SH, positive windspeed correlations are seen at 80°W through 40°E.

All significant subtropical jet latitude (altitude) correlations with MEIv2 in JJA (Fig. 8) are negative (positive) (i.e., poleward (downward) shifts of the jets during La Niña). Latitude correlations are significant in the NH from 120°E across the dateline to 100°W and 20–40°E; they are significant in the SH from160°E across the dateline to 120°W, 20–40°E, and 60–100°E. Altitude correlations are significant in the NH from about 140°E across the dateline to 80°W (excepting MERRA-2 and ERA-Interim at 160–180°E), and in the SH for all reanalyses only in 120–140°E but for some of the reanalyses from 100°E across the dateline to 140°W. NH subtropical jet windspeeds show significant negative correlations with MEIv2 (i.e., stronger windspeeds during La Niña) at about 160–80°W and significant positive correlations (i.e., weaker windspeeds during La Niña) at 140–160°E; windspeed correlations in the SH are significantly positive at 160°E across the dateline to 80°W, and significantly negative from 0–100°E.

Fig. 9 show significantly negative correlations of subtropical jet latitude with MEIv2 (i.e., poleward shifts during La Niña) in the NH except from 100°W through 20°E and at 140–160°E. In the SH, significant negative latitude correlations are seen in most of the region from 20°E across the dateline to 120°W, and significant positive correlations from 60–40°W. Strong negative windspeed correlations (i.e., stronger windspeeds during La Niña) are seen from 100°E across the dateline to 120°W in the NH, with significant positive correlations from 100–60°W.

While there were few months / seasons with significant correlations of MEIv2 with polar jet characteristics in the zonal mean (Fig. 5), Figs. 10 through 13 show numerous regions with strong correlations that vary by season. As emphasized by Manney and Hegglin (2018) for trend studies, this again highlights the importance of studying longitudinally resolved variations in jet dependencies on ENSO. Significant negative correlations with latitude in the NH occur over east Asia and the western Pacific (around 120–180°E) in DJF and MAM and over north America (about 120–140°W) in JJA. In the SH, significant negative correlations with latitude (poleward shifts during La Niña) are seen in DJF over most of 40°E across the Greenwich meridian and the dateline through 160°W, near the dateline in MAM, and around 60–100°E in SON. Altitude correlations are generally not significant in either hemisphere in JJA or SON. In DJF, significant positive correlations of MEIv2 with polar jet altitude (i.e., downward shift during La Niña) are seen in the NH from about 40°W to 100°E and in the SH from 40–80°E and 120°E across the dateline to 160°W; significant negative correlations are seen in the NH over North America (120–80°W). In MAM, significant positive altitude correlations (i.e., downward shifts during La Niña) are seen in the NH from 100°E across the dateline to 160°W, and in the SH from 20°E across the dateline to 160°W. The pattern of polar jet windspeed correlations with MEIv2 is typically negative (i.e., strengthening of windspeeds during La Niña) in the western hemisphere and positive (i.e., weakening of windspeeds during La Niña) in the eastern hemisphere, except in the NH in JJA when

correlations are weak/insignificant everywhere except just east of the Greenwich meridian. These windspeed correlations are significant in most of the NH western hemisphere in DJF and MAM, and in a smaller region over the eastern Pacific and western North America in SON. In the SH these windspeed correlations are strongest / most significant in JJA and SON but still significant in much of the western hemisphere in DJF and MAM. The persistent sign change with region in the windspeed correlations explains the lack of strong correlations in the zonal mean.

4. Conclusions and Discussion

A comprehensive view of the relationships of UT jet stream variability to ENSO is given. We present the analysis for three reanalyses to assess the robustness of the results, and examine the regional and seasonal variations starting with a daily 3D characterization of the jets. Relationships for subtropical and polar (eddy-driven) jets are evaluated separately.

La Niña and El Niño composites in relation to climatological and neutral conditions show the same qualitative patterns as La Niña / El Niño differences, indicating that La Niña and El Niño are indeed associated with opposite anomalies in the UT winds; examining La Niña / El Niño differences thus provides a complete view of the patterns of ENSO-related variability. Maps and cross-sections of composites for El Niño and La Niña and their differences show qualitatively very similar patterns for all the reanalyses, and show strong seasonal, regional, and hemispheric variability in the relationships of UT jets to ENSO as characterized by the MEIv2. Common patterns seen in these composites include:

- Tropical jets (both easterly and westerly) associated with monsoon and Walker circulations are generally stronger during La Niña than during El Niño.

- In most regions/seasons where the subtropical jets are strong and relatively zonal, their latitude is more poleward under La Niña conditions; this shift is pervasive enough to be apparent in the zonal mean in SH summer and fall and in all seasons (especially MAM and SON) in the NH.

- The poleward shift of the subtropical jets during La Niña is generally accompanied by an altitude decrease; in MAM all extratropical jets show a downward shift during La Niña.

- The patterns of mid-to-high latitude ENSO-related jet changes are complex and difficult to interpret, but an equatorward shift of the polar jet during La Niña is suggested in several regions in the NH.

- In the SH, the "transitional" jet that spirals in from the subtropical to the polar jet shows an equatorward shift during La Niña.

The strengthening and reduced variability of tropical jets during La Niña is consistent with previous studies showing strengthening of tropical circulations and "westerly ducts" (which allow propagation of Rossby waves across the equator) during La Niña (Julian and Chervin 1978; Horinouchi et al. 2000; Waugh and Polvani 2000; Bayr et al. 2014, and references therein). The patterns of anomalies in westerly jets (subtropical and polar) reported here are consistent with those shown by Spensberger and Spengler (2020).

To quantify the relationships of UT subtropical and polar jets to ENSO, we analyzed regional and seasonal correlations of subtropical and polar jet latitude, altitude, and windspeed with the MEIv2. Figures 14 and 15 provide a schematic summary of these results. The correlations are very consistent among the three reanalyses shown here (and, for 1979–2015, for the MERRA and CFSR/CFSv2 reanalyses, not shown): When any of the reanalyses shows a significant (at/over the 95% confidence level) correlation, the sign of the correlation agrees among all reanalyses

(indicated in Figures 14 and 15 by all boxes with three significant correlations showing a grey background and the sign in the lower right quadrant). Further, most periods/regions with a significant correlation in any of the reanalyses also have significant correlations in the other reanalyses (indicated in Figures 14 and 15 by the preponderance of boxes with three significant and consistent correlations over those with a smaller non-zero number of significant correlations). This is in contrast to the often large disagreement in trends for the same jets found by Manney and Hegglin (2018), and thus suggests that factors that may affect trends (e.g., differences in assimilation methods, in treatment of changes in observing systems, or in usage of data inputs) do not have the same sort of detrimental effect on this type of correlation analysis. This agreement provides confidence in the robustness of our results.

Correlations of ENSO with subtropical jet position are sufficiently consistent across large regions that most seasons show significant correlations in the zonal mean. Subtropical jet latitude is significantly negatively correlated with MEIv2 (that is, the jet is more poleward during La Niña conditions) in all seasons in both hemispheres, except in one of the reanalyses, MERRA-2, in DJF in the NH and MAM in the SH. Subtropical jet altitude is positively correlated with MEIv2 in all seasons in the NH and in DJF and MAM in the SH (downward shift during La Niña). Correlations of windspeed are less consistent, with significant positive correlations *[(weakening during La Niña)]* in the NH in DJF and MAM and in the SH in MAM and SON; the NH shows a significant negative correlation in SON. We can summarize the seasonal and regional correlations in Fig. 14 as follows:

- Significant correlations of subtropical jet latitude with MEIv2 are negative in both hemispheres (i.e., a poleward jet shift during La Niña), with exceptions in small regions in DJF (NH, 160–140°W), MAM (SH, 20°W to 20°E), and SON (SH, 60–40°W).

- Significant subtropical jet altitude correlations with MEIv2 are always positive (i.e., a downward jet shift during La Niña), and the altitude correlations in the regions with positive latitude correlations are not significant.

- Significant correlations of subtropical jet windspeed vary in sign, with mainly positive values in DJF and MAM in both hemispheres and in the SH western hemisphere in JJA and SON (i.e., weakening of jets during La Niña); negative correlations are seen in the NH surrounding the dateline in SON and in the SH eastern hemisphere in JJA and SON.

The localized region in DJF with a positive correlation between MEIv2 and NH jet latitude coincides with the region where Manney and Hegglin (2018) found a robust equatorward shift (indicative of tropical narrowing) over 1979–2015 of the NH (and SH) subtropical jet in that season; this appears consistent with the stronger dominance of La Niña they noted in the later years of that period. Similarly, the SH region with a positive correlation in MAM coincides with a region where Manney and Hegglin (2018) found a robust equatorward shift of the SH subtropical jet. Also, the few regions where Manney and Hegglin (2018) found robust poleward trends of the subtropical jet correspond to regions with negative MEIv2 / subtropical jet latitude correlations. (Conversely, there are significant correlations between MEIv2 and subtropical jet latitude at many times/regions where Manney and Hegglin (2018) found no significant trends in the subtropical jet latitude.) The positive correlations of subtropical jet altitude with ENSO are consistent with the expectation of a negative shift in jet altitude with increasing latitude (see Manney and Hegglin 2018, and references therein). Unlike the generally anti-correlated pattern between changes in subtropical jet latitude and altitude with ENSO variations, subtropical jet windspeed correlations do not show a consistent relationship to positive or negative correlations in subtropical jet position; however, the correlations are mostly positive (negative) in the western (eastern) hemisphere during winter.

Manney et al. (2020) showed significant positive (negative) correlations between the ASM anticyclone centroid latitude (altitude) and the subtropical jet, as well as significant negative correlations between the ASMA centroid latitude and ENSO, consistent with the subtropical jet results shown here.

Several previous studies have linked ENSO variations to changes in ozone transport near the subtropical jet that appear consistent with our results (Langford 1999; Lin et al. 2015; Olsen et al. 2019, and references therein); most recently, Olsen et al. (2019) showed that the region where ENSO has its strongest impact on tropospheric column ozone is in the 180°W to 135°W region, where the subtropical jet most frequently shows strong correlations with ENSO.

Correlations of MEIv2 with the polar jets (Fig. 15) are significant less frequently and cover smaller regions than those for the subtropical jets, resulting in few periods with significant correlations in the zonal mean. December in the SH is the only month that shows a significant correlation (negative) of polar jet latitude with MEIv2; Apr and MAM in the NH, and Jan, Mar, and MAM in the SH show significant (positive) altitude correlations with MEIv2; and Jan, Mar, and DJF in the NH and Aug, Dec, and DJF in the SH show significant windspeed correlations (all negative except in Dec in the SH). Significant correlations are more common in limited regions (Fig. 15):

- Significant latitude correlations are uncommon in the NH, with negative correlations (i.e., poleward jet shifts during La Niña) in DJF and MAM at 120–160°E and JJA at 120–80°W, and positive correlations (i.e., equatorward jet shifts during La Niña) in MAM at 120–100°W.

- In the SH, significant polar jet latitude correlations are seen in larger regions, with negative correlations from 40°E across the dateline through 160°W in DJF (and a more limited region near the dateline in MAM) and positive correlations in JJA and SON at 160–80°W.

- As was the case for the subtropical jet, significant altitude correlations are usually positive (i.e., downward shift during La Niña). These occur primarily in DJF and MAM, with few significant correlations in either hemisphere in JJA or SON.

- Polar jet windspeed correlations in both hemispheres tend to show a "dipole" pattern with negative correlations in the western hemisphere and positive ones in the eastern hemisphere. Most significant correlations are seen in SON and DJF in the NH and in JJA and SON in the SH.

Previous studies have shown impacts of tropical variability, including ENSO, on storm tracks and hence the UT mid-latitude westerly eddy-driven jet (what we call the PJ) (e.g., Li and Wettstein 2012; Schemm et al. 2016, 2018); this storm track variability projects strongly onto extra-tropical teleconnections (e.g., Wettstein and Wallace 2010). Because of the indirect nature and strong seasonality and regionality of tropical to extra-tropical teleconnections (e.g., Stan et al. 2017), limited regions of, and strong variability in, ENSO/PJ correlations are perhaps to be expected. Manney and Hegglin (2018) showed limited regions with robust changes in PJ characteristics, with the exception of a near global and near year-round increase in NH PJ altitude. The regions/seasons with robust PJ/ENSO correlations are not, in general, particularly well aligned with the regions/seasons with robust PJ trends, nor are the signs typically consistent when those regions do overlap; this indicates that those trends are not primarily driven by trends in ENSO; for the SH, this result is consistent with the meta-analysis of Waugh et al. (2015) showing SH jet latitude shifts are largely linked to effects of stratospheric ozone depletion rather than to SST variations.

The methods and characterization of jets used here are also being applied to study relationships of UT jets to other modes of variability, including the Quasi-biennial oscillation and the north Atlantic oscillation. We are also using these tools to study connections between the lower

stratospheric vortex and sub-vortex (see, e.g., Manney et al. 2014, for JETPAC view of subvortex climatology). Our comprehensive analysis of the relationships of interannual variability in UT jet streams to ENSO provides quantitative results, summarized above, that are valuable for assessing climate model representation and prediction of these features. Our study highlights the importance of seasonal and regional variability in these relationships. Because of the important roles the UT jets play, this information and future related studies will continue to help advance our understanding of current and future weather and climate.

Acknowledgments. We thank the Microwave Limb Sounder team at JPL, especially Brian Knosp and Luis Millán, for computational, data processing, management, and analysis support; Mark Olsen and Ted Shepherd for helpful discussions / comments; NASA's GMAO, for providing their assimilated data products; GLM and ZDL were partially supported by the JPL Microwave Limb Sounder team under a JPL subcontract to NWRA and under NASA grant NNX14AE85G. The datasets used/produced are publicly available, as follows:

- MERRA-2: https://disc.sci.gsfc.nasa.gov/uui/datasets?keywords=%22MERRA-2%22
- ERA-I: http://apps.ecmwf.int/datasets/
- JRA-55: Through NCAR RDA at http://dx.doi.org/10.5065/D6HH6H41
- MEIv2 indices: https://www.esrl.noaa.gov/psd/enso/mei/

References

Bai, K., N.-B. Chang, and W. Gao, 2016: Quantification of relative contribution of Antarctic ozone depletion to increased austral extratropical precipitation during 1979–2013. *J. Geophys. Res.*, **121**, 1459–1474, doi:10.1002/2015JD024247, URL http://dx.doi.org/10.1002/2015JD024247.

Barnes, E. A., and J. A. Screen, 2015: The impact of Arctic warming on the midlatitude jet-stream: Can it? has it? will it? *Wiley Interdisciplinary Reviews: Climate Change*, **6 (3)**, 277–286.

Bayr, T., D. Dommenget, T. Martin, and S. B. Power, 2014: The eastward shift of the Walker Circulation in response to global warming and its relationship to ENSO variability. *Clim. Dyn.*, **43 (9-10)**, 2747–2763.

Bloom, S. C., L. L. Takacs, A. M. da Silva, and D. Ledvina, 1996: Data assimilation using incremental analysis updates. *Mon. Weather Rev.*, **124**, 1256–1271.

Bollasina, M. A., Y. Ming, V. Ramaswamy, M. D. Schwarzkopf, and V. Naik, 2014: Contribution of local and remote anthropogenic aerosols to the twentieth century weakening of the South Asian Monsoon. *Geophys. Res. Lett.*, **41 (2)**, 680–687, doi:10.1002/2013GL058183, URL https://agupubs.onlinelibrary.wiley.com/doi/abs/10.1002/2013GL058183, https://agupubs.onlinelibrary.wiley.com/doi/pdf/10.1002/2013GL058183.

Bombardi, R. J., V. Moron, and J. S. Goodnight, 2020: Detection, variability, and predictability of monsoon onset and withdrawal dates: A review. *Int. J. Clim.*, **40 (2)**, 641–667, doi:10.1002/joc.6264, URL https://rmets.onlinelibrary.wiley.com/doi/abs/10.1002/joc.6264.

Byrne, N. J., T. G. Shepherd, and I. Polichtchouk, 2019: Subseasonal-to-seasonal predictability of the Southern Hemisphere eddy-driven jet during Austral spring and early summer. *J. Geophys. Res.*, **124 (13)**, 6841–6855, doi:10.1029/2018JD030173, URL https://agupubs.onlinelibrary.wiley.com/doi/abs/10.1029/2018JD030173.

Byrne, N. J., T. G. Shepherd, T. Woollings, and R. A. Plumb, 2017: Nonstationarity in Southern Hemisphere Climate Variability Associated with the Seasonal Breakdown of the Stratospheric Polar Vortex. *J. Clim.*, **30 (18)**, 7125–7139, doi:10.1175/JCLI-D-17-0097.1, URL https:

//doi.org/10.1175/JCLI-D-17-0097.1, https://journals.ametsoc.org/jcli/article-pdf/30/18/7125/4769817/jcli-d-17-0097_1.pdf.

Calvo, N., R. R. Garcia, W. J. Randel, and D. R. Marsh, 2010: Dynamical Mechanism for the Increase in Tropical Upwelling in the Lowermost Tropical Stratosphere during Warm ENSO Events. *J. Atmos. Sci.*, **67 (7)**, 2331–2340, doi:10.1175/2010JAS3433.1, URL https://doi.org/10.1175/2010JAS3433.1, https://journals.ametsoc.org/jas/article-pdf/67/7/2331/3518461/2010jas3433_1.pdf.

Chen, G., J. Lu, and D. M. W. Frierson, 2008: Phase Speed Spectra and the Latitude of Surface Westerlies: Interannual Variability and Global Warming Trend. *J. Clim.*, **21 (22)**, 5942–5959, doi:10.1175/2008JCLI2306.1, URL https://doi.org/10.1175/2008JCLI2306.1, https://journals.ametsoc.org/jcli/article-pdf/21/22/5942/3949667/2008jcli2306_1.pdf.

Dee, D. P., and Coauthors, 2011a: The ERA-Interim reanalysis: configuration and performance of the data assimilation system. *Q. J. R. Meteorol. Soc.*, **137**, 553–597.

Dee, D. P., and Coauthors, 2011b: The ERA-Interim reanalysis: configuration and performance of the data assimilation system. *Q. J. R. Meteorol. Soc.*, **137**, 553–597.

Delworth, T. L., and F. Zeng, 2014: Regional rainfall decline in Australia attributed to anthropogenic greenhouse gases and ozone levels. *Nature Geosci.*, **7**, 583–587.

Diallo, M., and Coauthors, 2019: Structural changes in the shallow and transition branch of the Brewer–Dobson circulation induced by El Niño. *Atmos. Chem. Phys.*, **19 (1)**, 425–446, doi:10.5194/acp-19-425-2019, URL https://acp.copernicus.org/articles/19/425/2019/.

Díaz, L. B., and C. S. Vera, 2017: Austral summer precipitation interannual variability and trends over Southeastern South America in CMIP5 models. *Int. J. Clim.*, **37 (S1)**, 681–

695, doi:https://doi.org/10.1002/joc.5031, URL https://rmets.onlinelibrary.wiley.com/doi/abs/10.1002/joc.5031, https://rmets.onlinelibrary.wiley.com/doi/pdf/10.1002/joc.5031.

Domeisen, D. I., C. I. Garfinkel, and A. H. Butler, 2019: The teleconnection of El Niño Southern Oscillation to the stratosphere. *Rev. Geophys.*, **57 (1)**, 5–47, doi:10.1029/2018RG000596, URL https://agupubs.onlinelibrary.wiley.com/doi/abs/10.1029/2018RG000596.

Ebita, A., and Coauthors, 2011: The Japanese 55-year Reanalysis "JRA-55": An interim report. *SOLA*, **7**, 149–152.

Elfron, B., and R. J. Tibshirani, 1993: *An Introduction to the Bootstrap*. No. 57, Monographs on Statistics and Applied Probability, Chapman & Hall.

Francis, J. A., 2017: Why are Arctic linkages to extreme weather still up in the air? *Bull. Am. Meteor. Soc.*, **98 (12)**, 2551–2557, doi:10.1175/BAMS-D-17-0006.1, URL https://doi.org/10.1175/BAMS-D-17-0006.1.

Fujiwara, M., and Coauthors, 2017: Introduction to the SPARC Reanalysis Intercomparison Project (S-RIP) and overview of the reanalysis systems. *Atmos. Chem. Phys.*, **17**, 1417–1452, doi:10.5194/acp-17-1417-2017, URL www.atmos-chem-phys.net/17/1417/2017/.

Garfinkel, C. I., D. W. Waugh, and L. M. Polvani, 2015: Recent Hadley cell expansion: The role of internal atmospheric variability in reconciling modeled and observed trends. *Geophys. Res. Lett.*, **42 (24)**.

Gelaro, R., and Coauthors, 2017: The Modern-Era Retrospective Analysis for Research and Applications, Version-2 (MERRA-2). *J. Clim.*, **30**, 5419–5454, doi:doi:10.1175/JCLI-D-16-0758.1.

Global Modeling and Assimilation Office (GMAO), 2015: Merra-2 inst3_3d_asm_nv: 3d, 3-hourly,instantaneous, model-level, assimilation, assimilated meteorological fields v5.12.4,

greenbelt, md, usa, Goddard Earth Sciences Data and Information Services Center (GES DISC), accessed 1 november 2015. doi:10.5067/WWQSXQ8IVFW8.

Grise, K. M., S. M. Davis, P. W. Staten, and O. Adam, 2018: Regional and Seasonal Characteristics of the Recent Expansion of the Tropics. *J. Clim.*, **31 (17)**, 6839–6856, doi:10.1175/JCLI-D-18-0060.1, URL https://doi.org/10.1175/JCLI-D-18-0060.1, https://journals.ametsoc.org/jcli/article-pdf/31/17/6839/4696875/jcli-d-18-0060_1.pdf.

Grise, K. M., and Coauthors, 2019: Recent tropical expansion: Natural variability or forced response? *J. Clim.*, **32 (5)**, 1551–1571, doi:10.1175/JCLI-D-18-0444.1, URL https://journals.ametsoc.org/view/journals/clim/32/5/jcli-d-18-0444.1.xml.

Grotjahn, R., and Coauthors, 2016: North American extreme temperature events and related large scale meteorological patterns: a review of statistical methods, dynamics, modeling, and tr ends. *Clim. Dyn.*, **46 (3)**, 1151–1184, doi:10.1007/s00382-015-2638-6, URL https://doi.org/10.1007/s00382-015-2638-6.

Harnik, N., C. I. Garfinkel, and O. Lachmy, 2016: The influence of jet stream regime on extreme weather events. *in "Dynamics and Predictability of Large-Scale, High-Impact Weather and Climate Events"*, **2**, 79–94.

Held, I. M., and P. J. Phillips, 1990: A barotropic model of the interaction between the Hadley cell and a Rossby wave. *J. Atmos. Sci.*, **47**, 856–869.

Held, I. M., M. Ting, and H. Wang, 2002: Northern winter stationary waves: Theory and modeling. *J. Clim.*, **15**, 2125–2144.

Homeyer, C. R., G. L. Manney, L. F. M. A. C. Boothe, T. Xian, M. A. Olsen, M. J. Schwartz, Z. D. Lawrence, and K. Wargan, 2020: Extratropical upper troposphere and lower stratosphere

(ExUTLS). *S-RIP Final Report*, M. Fujiwara, G. L. Manney, L. J. Grey, and J. S. Wright, Eds., chap. 7, in press.

Horinouchi, T., F. Sassi, and B. A. Boville, 2000: Synoptic-scale Rossby waves and the geographic distribution of lateral transport routes between the tropics and the extratropics in the lower stratosphere. *J. Geophys. Res.*, **105**, 26,579–26,592.

Hoskins, B. J., and P. J. Valdes, 1990: On the existence of storm tracks. *J. Atmos. Sci.*, **47**, 1854–1864.

Huang, D.-Q., J. Zhu, Y.-C. Zhang, J. Wang, and X.-Y. Kuang, 2015: The impact of the East Asian subtropical jet and polar front jet on the frequency of spring persistent rainfall over Southern China in 1997–2011. *J. Clim.*, **28**, 6054–6066, doi:10.1175/JCLI-D-14-00641.1.

Hudson, R. D., 2012: Measurements of the movement of the jet streams at mid-latitudes, in the Northern and Southern Hemispheres, 1979 to 2010. *Atmos. Chem. Phys.*, **12**, 7797–7808.

Hulme, M., and N. Tosdevin, 1989: The tropical easterly jet and Sudan rainfall: A review. *Theor. Appl. Clim.*, **39 (4)**, 179–187, URL https://doi.org/10.1007/BF00867945.

Ju, J., and J. Slingo, 1995: The Asian summer monsoon and ENSO. *Q. J. R. Meteorol. Soc.*, **121 (525)**, 1133–1168, doi:10.1002/qj.49712152509, URL https://rmets.onlinelibrary.wiley.com/doi/abs/10.1002/qj.49712152509, https://rmets.onlinelibrary.wiley.com/doi/pdf/10.1002/qj.49712152509.

Julian, P., and R. Chervin, 1978: A study of the Southern Oscillation and Walker circulation phenomenon. *Mon. Weather Rev.*, **106**, 1433–1451.

Kang, S. M., L. M. Polvani, J. C. Fyfe, and M. Sigmond, 2011: Impact of polar ozone depletion on subtropical precipitation. *Science*, **332 (6032)**, 951–954, doi:10.1126/science.

1202131, URL http://science.sciencemag.org/content/332/6032/951, http://science.sciencemag.org/content/332/6032/951.full.pdf.

Kelly, P., L. R. Leung, K. Balaguru, W. Xu, B. Mapes, and B. Soden, 2018: Shape of Atlantic tropical cyclone tracks and the Indian monsoon. *Geophys. Res. Lett.*, **45 (19)**, 10,746–10,755, doi:10.1029/2018GL080098, URL https://agupubs.onlinelibrary.wiley.com/doi/abs/10.1029/2018GL080098, https://agupubs.onlinelibrary.wiley.com/doi/pdf/10.1029/2018GL080098.

Kobayashi, S., and Coauthors, 2015: The JRA-55 reanalysis: General specification and basic characteristics. *J. Meteor. Soc. Japan*, **93**, doi:10.2151/jmsj.2015-001.

Kolstad, E. W., T. Breiteig, and A. A. Scaife, 2010: The association between stratospheric weak polar vortex events and cold air outbreaks in the Northern Hemisphere. *Q. J. R. Meteorol. Soc.*, **136**, 886–893.

Langford, A., 1999: Stratosphere-troposphere exchange at the subtropical jet: Contribution to the tropospheric ozone budget at midlatitudes. *Geophys. Res. Lett.*, **26**, 2449–2452.

Lawrence, Z. D., and G. L. Manney, 2020: Does the Arctic Stratospheric Polar Vortex Exhibit Signs of Preconditioning Prior to Sudden Stratospheric Warmings? *J. Atmos. Sci.*, **77 (2)**, 611–632, doi:10.1175/JAS-D-19-0168.1, URL https://doi.org/10.1175/JAS-D-19-0168.1, https://journals.ametsoc.org/jas/article-pdf/77/2/611/4917744/jas-d-19-0168_1.pdf.

Lawrence, Z. D., G. L. Manney, and K. Wargan, 2018: Reanalysis intercomparisons of stratospheric polar processing diagnostics. *Atmos. Chem. Phys.*, **18**, 13 547–13 579, doi:10.5194/acp-18-13547-2018.

Lee, S., and H.-K. Kim, 2003: The dynamical relationship betweem subtropical and eddy-driven jets. *J. Atmos. Sci.*, **60**, 1490–1503.

673 Li, C., and J. J. Wettstein, 2012: Thermally driven and eddy-driven jet variability in reanalysis. *J.*
674 *Clim.*, **25**, 1587–1596.

675 Li, T., B. Wang, B. Wu, T. Zhou, C.-P. Chang, and R. Zhang, 2017: Theories on formation of an
676 anomalous anticyclone in western North Pacific during El Niño: A review. *J. Meteorol. Res.*,
677 **31 (6)**, 987–1006, URL https://doi.org/10.1007/s13351-017-7147-6.

678 Lin, M., A. M. Fiore, L. W. Horowitz, A. O. Langford, S. J. Oltmans, D. Tarasick, and H. E.
679 Rieder, 2015: Climate variability modulates western US ozone air quality in spring via deep
680 stratospheric intrusions. *Nature Commun.*, **6**.

681 Lin, M., L. W. Horowitz, S. J. Oltmans, A. M. Fiore, and S. Fan, 2014: Tropospheric ozone trends
682 at Mauna Loa Observatory tied to decadal climate variability. *Nature Geosci.*, **7**, 136–143.

683 Long, C. S., M. Fujiwara, S. Davis, D. M. Mitchell, and C. J. Wright, 2017: Climatology and
684 interannual variability of dynamic variables in multiple reanalyses evaluated by the SPARC
685 Reanalysis Intercomparison Project (S-RIP). *Atmos. Chem. Phys.*, **17**, 14,593–14,629, URL
686 https://doi.org/10.5194/acp-17-14593-2017.

687 Lorenz, D. J., and E. T. DeWeaver, 2007: Tropopause height and zonal wind response to
688 global warming in the IPCC scenario integrations. *J. Geophys. Res.*, **112**, D10119, doi:
689 10.1029/2006JD008087.

690 Lucas, C., and H. Nguyen, 2015: Regional characteristics of tropical expansion and the role of
691 climate variability. *Journal of Geophysical Research: Atmospheres*, **120 (14)**, 6809–6824, doi:
692 10.1002/2015JD023130, URL http://dx.doi.org/10.1002/2015JD023130, 2015JD023130.

693 Lucas, C., H. Nguyen, and B. Timbal, 2012: An observational analysis of southern hemisphere
694 tropical expansion. *Journal of Geophysical Research: Atmospheres*, **117 (D17)**, n/a–n/a, doi:
695 10.1029/2011JD017033, URL http://dx.doi.org/10.1029/2011JD017033, d17112.

696 Lucas, C., B. Timbal, and H. Nguyen, 2014: The expanding tropics: A critical assessment of the
697 observational and modeling studies. *WIRES: Climate Change*, **5**, 89–112, doi:10.1002/wcc.251,
698 URL http://dx.doi.org/10.1002/wcc.251.

699 Maher, P., M. E. Kelleher, P. G. Sansom, and J. Methven, 2019: Is the subtropical jet shift-
700 ing poleward? *Clim. Dyn.*, doi:10.1007/s00382-019-05084-6, URL https://doi.org/10.1007/
701 s00382-019-05084-6.

702 Mann, M. E., S. Rahmstorf, K. Kornhuber, B. A. Steinman, S. K. Miller, and D. Coumou, 2017:
703 Influence of anthropogenic climate change on planetary wave resonance and extreme weather
704 events. *Nature Scientific Reports*, **7**, doi:10.1038/srep45242.

705 Manney, G. L., and M. I. Hegglin, 2018: Seasonal and regional variations in long-term changes in
706 upper tropospheric jets from reanalyses. *J. Clim.*, **31**, 423–448.

707 Manney, G. L., M. I. Hegglin, W. H. Daffer, M. J. Schwartz, M. L. Santee, and S. Pawson, 2014:
708 Climatology of upper tropospheric/lower stratospheric (UTLS) jets and tropopauses in MERRA.
709 *J. Clim.*, **27**, 3248–3271.

710 Manney, G. L., Z. D. Lawrence, M. L. Santee, M. J. Schwartz, and K. Wargan, 2020: A moments
711 view of climatology and variability of the Asian monsoon anticyclone, submitted to *J. Clim.*,
712 2020.

Manney, G. L., and Coauthors, 2011: Jet characterization in the upper troposphere/lower stratosphere (UTLS): Applications to climatology and transport studies. *Atmos. Chem. Phys.*, **11**, 6115–6137.

Manney, G. L., and Coauthors, 2017: Reanalysis comparisons of upper tropospheric/lower stratospheric jets and multiple tropopauses. *Atmos. Chem. Phys.*, 11 541–11 566.

Martineau, P., J. S. Wright, N. Zhu, and M. Fujiwara, 2018: Zonal-mean data set of global atmospheric reanalyses on pressure levels. *Earth Sys. Sci. Data*, **10 (4)**, 1925–1941, doi: 10.5194/essd-10-1925-2018, URL https://www.earth-syst-sci-data.net/10/1925/2018/.

McLandress, C., T. G. Shepherd, J. F. Scinocca, D. A. Plummer, M. Sigmond, A. I. Jonsson, and M. C. Reader, 2011: Separating the dynamical effects of climate change and ozone depletion. Part II: Southern Hemisphere troposphere. *J. Clim.*, **24**, 1850–1868.

Minschwaner, K., and Coauthors, 2015: Signature of a tropical Pacific cyclone in the composition of the upper troposphere over Socorro, NM. *Geophys. Res. Lett.*, **42 (21)**, 9530–9537, doi: 10.1002/2015GL065824, URL http://dx.doi.org/10.1002/2015GL065824, 2015GL065824.

Nakamura, H., T. Sampe, Y. Tanimoto, and A. Shimpo, 2004: *Observed Associations Among Storm Tracks, Jet Streams and Midlatitude Oceanic Fronts*, 329–345. American Geophysical Union (AGU), doi:https://doi.org/10.1029/147GM18, URL https://agupubs.onlinelibrary.wiley.com/doi/abs/10.1029/147GM18, https://agupubs.onlinelibrary.wiley.com/doi/pdf/10.1029/147GM18.

Olsen, M. A., G. L. Manney, and J. Liu, 2019: The ENSO and QBO impact on ozone variability and stratosphere-troposphere exchange relative to the subtropical jets. *J. Geophys. Res.*,

124 (13), 7379–7392, doi:10.1029/2019JD030435, URL https://agupubs.onlinelibrary.wiley.com/doi/abs/10.1029/2019JD030435.

Olsen, M. A., K. Wargan, and S. Pawson, 2016: Tropospheric column ozone response to ENSO in GEOS-5 assimilation of OMI and MLS ozone data. *Atmos. Chem. Phys.*, **16**, 7091–7103, doi:10.5194/acp-16-7091-2016, URL http://www.atmos-chem-phys.net/16/7091/2016/.

Oman, L. D., J. R. Ziemke, A. R. Douglass, D. W. Waugh, C. Lang, J. M. Rodriguez, and J. E. Nielsen, 2011: The response of tropical tropospheric ozone to ENSO. *Geophys. Res. Lett.*, **38 (13)**, doi:https://doi.org/10.1029/2011GL047865, URL https://agupubs.onlinelibrary.wiley.com/doi/abs/10.1029/2011GL047865, https://agupubs.onlinelibrary.wiley.com/doi/pdf/10.1029/2011GL047865.

Overland, J. E., and Coauthors, 2016: Nonlinear response of mid-latitude weather to the changing Arctic. *Nature Climate Change*, **6 (11)**, 992–999.

Peña-Ortiz, C., D. Gallego, P. Ribera, P. Ordonez, and M. D. C. Alvarez-Castro, 2013: Observed trends in the global jet stream characteristics during the second half of the 20th century. *J. Geophys. Res.*, **118 (7)**, 2702–2713, doi:10.1002/jgrd.50305, URL http://dx.doi.org/10.1002/jgrd.50305.

Politis, D. N., and J. P. Romano, 1994: The stationary bootstrap. *Journal of the American Statistical Association*, **89 (428)**, 1303–1313, URL http://www.jstor.org/stable/2290993.

Price, C., L. Stone, A. Huppert, B. Rajagopalan, and P. Alpert, 1998: A possible link between El Niño and precipitation in Israel. *Geophys. Res. Lett.*, **25**, 3963–3966, doi:10.1029/1998GL900098, URL http://dx.doi.org/10.1029/1998GL900098.

Raible, C. C., U. Luksch, and K. Fraedrich, 2004: Precipitation and Northern Hemisphere regimes. *Atmos. Sci. Lett.*, **5**, 43–55, doi:10.1016/j.atmoscilet.2003.12.001, URL http://dx.doi.org/10.1016/j.atmoscilet.2003.12.001.

Randel, W. J., and Coauthors, 2009: An update of observed stratospheric temperature trends. *J. Geophys. Res.*, **114**, D02107, doi:10.1029/2008JD010421.

Rasmusson, E. M., and T. H. Carpenter, 1982: Variations in Tropical Sea Surface Temperature and Surface Wind Fields Associated with the Southern Oscillation/El Niño. *Mon. Weather Rev.*, **110 (5)**, 354–384, doi:10.1175/1520-0493(1982)110⟨0354:VITSST⟩2.0.CO;2, URL https://doi.org/10.1175/1520-0493(1982)110⟨0354:VITSST⟩2.0.CO;2, https://journals.ametsoc.org/mwr/article-pdf/110/5/354/4167514/1520-0493(1982)110_0354_vitsst_2_0_co_2.pdf.

RavindraBabu, S., M. Venkat Ratnam, G. Basha, and B. Krishnamurthy, 2019: Indian summer monsoon onset signatures on the tropical tropopause layer. *Atmos. Sci. Lett.*, **20 (3)**, e884, doi:10.1002/asl.884, URL https://rmets.onlinelibrary.wiley.com/doi/abs/10.1002/asl.884, https://rmets.onlinelibrary.wiley.com/doi/pdf/10.1002/asl.884.

Rienecker, M. M., and Coauthors, 2011: MERRA: NASA's Modern-Era Retrospective Analysis for Research and Applications. *J. Clim.*, **24**, 3624–3648.

Saha, S., and Coauthors, 2010: The NCEP Climate Forecast System Reanalysis. *Bull. Am. Meteor. Soc.*, **91**, 1015–1057.

Saha, S., and Coauthors, 2014: The NCEP Climate Forecast System Version 2. *J. Clim.*, **27**, 2185–2208.

Scaife, A. A., C. K. Folland, L. V. Alexander, A. Moberg, and J. R. Knight, 2008: European Climate Extremes and the North Atlantic Oscillation. *J. Clim.*, **21 (1)**, 72–83, doi:10.1175/

2007JCLI1631.1, URL https://doi.org/10.1175/2007JCLI1631.1, https://journals.ametsoc.org/jcli/article-pdf/21/1/72/3940170/2007jcli1631_1.pdf.

Schemm, S., L. M. Ciasto, C. Li, and N. G. Kvamstø, 2016: Influence of tropical Pacific sea surface temperature on the genesis of Gulf Stream cyclones. *J. Atmos. Sci.*, **73 (10)**, 4203–4214, doi:10.1175/JAS-D-16-0072.1, URL https://journals.ametsoc.org/view/journals/atsc/73/10/jas-d-16-0072.1.xml.

Schemm, S., G. Rivière, L. M. Ciasto, and C. Li, 2018: Extratropical cyclogenesis changes in connection with tropospheric ENSO teleconnections to the North Atlantic: Role of stationary and transient waves. *J. Atmos. Sci.*, **75 (11)**, 3943–3964, doi:10.1175/JAS-D-17-0340.1, URL https://journals.ametsoc.org/view/journals/atsc/75/11/jas-d-17-0340.1.xml.

Schiemann, R., D. Lüthi, and C. Schar, 2009: Seasonality and interannual variability of the westerly jet in the Tibetan Plateau region. *J. Clim.*, **22**, 2940–2957.

Shaman, J., and E. Tziperman, 2007: Summertime ENSO–North African–Asian jet teleconnection and implications for the Indian monsoons. *Geophys. Res. Lett.*, **34 (11)**, doi:https://doi.org/10.1029/2006GL029143, URL https://agupubs.onlinelibrary.wiley.com/doi/abs/10.1029/2006GL029143, https://agupubs.onlinelibrary.wiley.com/doi/pdf/10.1029/2006GL029143.

Shapiro, M. A., H. Wernli, N. A. Bond, and R. Langland, 2001: The influence of the 1997–99 El Niño Southern Oscillation on extratropical baroclinic life cycles over the eastern North Pacific. *Q. J. R. Meteorol. Soc.*, **127 (572)**, 331–342, doi:https://doi.org/10.1002/qj.49712757205, URL https://rmets.onlinelibrary.wiley.com/doi/abs/10.1002/qj.49712757205, https://rmets.onlinelibrary.wiley.com/doi/pdf/10.1002/qj.49712757205.

Shepherd, T. G., 2016: Effects of a warming Arctic. *Science*, **353 (6303)**, 989–990, doi: 10.1126/science.aag2349, URL http://science.sciencemag.org/content/353/6303/989, http://science.sciencemag.org/content/353/6303/989.full.pdf.

Spensberger, C., and T. Spengler, 2020: Feature-Based Jet Variability in the Upper Troposphere. *J. Clim.*, **33 (16)**, 6849–6871, doi:10.1175/JCLI-D-19-0715.1, URL https://doi.org/10.1175/JCLI-D-19-0715.1, https://journals.ametsoc.org/jcli/article-pdf/33/16/6849/4965335/jclid190715.pdf.

Stan, C., D. M. Straus, J. S. Frederiksen, H. Lin, E. D. Maloney, and C. Schumacher, 2017: Review of tropical-extratropical teleconnections on intraseasonal time scales. *Rev. Geophys.*, **55 (4)**, 902–937, doi:https://doi.org/10.1002/2016RG000538, URL https://agupubs.onlinelibrary.wiley.com/doi/abs/10.1002/2016RG000538, https://agupubs.onlinelibrary.wiley.com/doi/pdf/10.1002/2016RG000538.

Staten, P. W., K. M. Grise, and S. M. Davis, 2016: The width of the tropics: Climate variations and their impacts. *SPARC Newsletter*, **46**, 26–31.

Strong, C., and R. E. Davis, 2007: Winter jet stream trends over the Northern Hemisphere. *Q. J. R. Meteorol. Soc.*, **133**, 2109–2115.

Strong, C., and R. E. Davis, 2008: Variability in the position and strength of winter jet stream cores related to Northern Hemisphere teleconnections. *J. Clim.*, **21**, 584–592.

Tanaka, D., T. Iwasaki, S. Uno, M. Ujie, and K. Miyazaki, 2004a: Eliassen-Palm flux diagnosis based on isentropic representation. *J. Atmos. Sci.*, **61**, 2370–2383.

Tanaka, H., N. Ishizaki, and A. Kitoh, 2004b: Trend and interannual variability of Walker, monsoon and Hadley circulations defined by velocity potential in the upper troposphere. *Tellus A*,

56 (3), 250–269, doi:10.3402/tellusa.v56i3.14410, URL https://doi.org/10.3402/tellusa.v56i3.14410, https://doi.org/10.3402/tellusa.v56i3.14410.

Tegtmeier, S., and Coauthors, 2020a: Temperature and tropopause characteristics from reanalyses data in the tropical tropopause layer. *Atmos. Chem. Phys.*, **20 (2)**, 753–770, doi:10.5194/acp-20-753-2020, URL https://www.atmos-chem-phys.net/20/753/2020/.

Tegtmeier, S., and Coauthors, 2020b: Tropical troposphere layer. *S-RIP Final Report*, M. Fujiwara, G. L. Manney, L. J. Grey, and J. S. Wright, Eds., chap. 8, in press.

Thompson, D. W., S. Solomon, P. J. Kushner, M. H. Grise, and D. J. Karoly, 2011: Signatures of the Antarctic ozone hole in Southern Hemisphere surface climate change. *Nature Geoscience*, **4**, 741–749.

Tweedy, O. V., D. W. Waugh, W. J. Randel, M. Abalos, L. D. Oman, and D. E. Kinnison, 2018: The impact of Boreal summer ENSO events on tropical lower stratospheric ozone. *J. Geophys. Res.*, **123 (17)**, 9843–9857, doi:10.1029/2018JD029020, URL https://agupubs.onlinelibrary.wiley.com/doi/abs/10.1029/2018JD029020, https://agupubs.onlinelibrary.wiley.com/doi/pdf/10.1029/2018JD029020.

Uccellini, L. W., and D. R. Johnson, 1979: The Coupling of Upper and Lower Tropospheric Jet Streaks and Implications for the Development of Severe Convective Storms. *Mon. Weather Rev.*, **107 (6)**, 682–703, doi:10.1175/1520-0493(1979)107⟨0682:TCOUAL⟩2.0.CO;2, URL https://doi.org/10.1175/1520-0493(1979)107⟨0682:TCOUAL⟩2.0.CO;2, https://journals.ametsoc.org/mwr/article-pdf/107/6/682/4166314/1520-0493(1979)107_0682_tcoual_2_0_co_2.pdf.

Waugh, D. W., C. I. Garfinkel, and L. M. Polvani, 2015: Drivers of the recent tropical expansion in the Southern Hemisphere: Changing SSTs or ozone depletion? *J. Clim.*, **28**, 6581–6586,

842 doi:10.1175/JCLI-D-15-0138.1, URL http://dx.doi.org/10.1175/JCLI-D-15-0138.1.

843 Waugh, D. W., and L. M. Polvani, 2000: Climatology of intrusions into the tropical upper tropo-
844 sphere. *Geophys. Res. Lett.*, **27**, 3857–3860.

845 Waugh, D. W., and Coauthors, 2018: Revisiting the Relationship among Metrics of Tropical Ex-
846 pansion. *J. Clim.*, **31 (18)**, 7565–7581, doi:10.1175/JCLI-D-18-0108.1, URL https://doi.org/
847 10.1175/JCLI-D-18-0108.1, https://journals.ametsoc.org/jcli/article-pdf/31/18/7565/4710799/
848 jcli-d-18-0108_1.pdf.

849 Wettstein, J. J., and J. M. Wallace, 2010: Observed patterns of month-to-month storm-track vari-
850 ability and their relationship to the background flow. *J. Atmos. Sci.*, **67 (5)**, 1420–1437, doi:10.
851 1175/2009JAS3194.1, URL https://journals.ametsoc.org/view/journals/atsc/67/5/2009jas3194.
852 1.xml.

853 Williams, L. N., S. Lee, and S.-W. Son, 2007: Dynamics of the Southern Hemisphere spiral jet. *J.*
854 *Atmos. Sci.*, **64**, 548–563.

855 Winters, A. C., L. F. Bosart, and D. Keyser, 2019: Antecedent North Pacific jet regimes con-
856 ducive to the development of continental U.S. extreme temperature events during the cool
857 season. *Weather and Forecasting*, **34 (2)**, 393–414, doi:10.1175/WAF-D-18-0168.1, URL
858 https://doi.org/10.1175/WAF-D-18-0168.1.

859 Wolter, K., and M. S. Timlin, 2011: El Niño/Southern Oscillation behaviour since 1871 as di-
860 agnosed in an extended multivariate ENSO index (MEI.ext). *Intl. J. Clim.*, **31**, 1074–1087,
861 doi:10.1002/joc.2336, URL http://dx.doi.org/10.1002/joc.2336.

Wright, J. S., and Coauthors, 2020: Differences in tropical high clouds among reanalyses: origins and radiative impacts. *Atmos. Chem. Phys.*, **20 (14)**, 8989–9030, doi:10.5194/acp-20-8989-2020, URL https://acp.copernicus.org/articles/20/8989/2020/.

Xian, T., and C. R. Homeyer, 2019: Global tropopause altitudes in radiosondes and reanalyses. *Atmos. Chem. Phys.*, **19**, 5661–5678.

Xie, Z., Y. Du, and S. Yang, 2015: Zonal extension and retraction of the subtropical westerly jet stream and evolution of precipitation over East Asia and the Western Pacific. *J. Clim.*, **28**, 6783–6798, doi:10.1175/JCLI-D-14-00649.1.

Yan, X., P. Konopka, F. Ploeger, M. Tao, R. Müller, M. L. Santee, J. Bian, and M. Riese, 2018: El Niño Southern Oscillation influence on the Asian summer monsoon anticyclone. *Atmos. Chem. Phys.*, **18 (11)**, 8079–8096, doi:10.5194/acp-18-8079-2018, URL https://www.atmos-chem-phys.net/18/8079/2018/.

Yulaeva, E., and J. M. Wallace, 1994: The Signature of ENSO in Global Temperature and Precipitation Fields Derived from the Microwave Sounding Unit. *J. Clim.*, **7 (11)**, 1719–1736, doi:10.1175/1520-0442(1994)007⟨1719:TSOEIG⟩2.0.CO;2, URL https://doi.org/10.1175/1520-0442(1994)007⟨1719:TSOEIG⟩2.0.CO;2, https://journals.ametsoc.org/jcli/article-pdf/7/11/1719/4698278/1520-0442(1994)007_1719_tsoeig_2_0_co_2.pdf.

Zeng, G., and J. A. Pyle, 2005: Influence of El Niño Southern Oscillation on stratosphere/troposphere exchange and the global tropospheric ozone budget. *Geophys. Res. Lett.*, **32**, L01814, doi:10.1029/2004GL021353.

Zhang, R., A. Sumi, and M. Kimoto, 1999: A diagnostic study of the impact of El Niño on the precipitation in china. *Adv. Atmos. Sci.*, **16 (2)**, 229–241, URL https://doi.org/10.1007/

BF02973084.

Zhang, T., A. Hoell, J. Perlwitz, J. Eischeid, D. Murray, M. Hoerling, and T. M. Hamill, 2019: Towards probabilistic multivariate ENSO monitoring. *Geophys. Res. Lett.*, **46 (17-18)**, 10 532–10 540, doi:10.1029/2019GL083946, URL https://agupubs.onlinelibrary.wiley.com/doi/abs/10.1029/2019GL083946, https://agupubs.onlinelibrary.wiley.com/doi/pdf/10.1029/2019GL083946.

Zhao, Y., X. Yu, J. Yao, and X. Dong, 2018: Evaluation of the subtropical westerly jet and its effects on the projected summer rainfall over central Asia using multi-CMIP5 models. *Int. J. Clim.*, **38 (S1)**, e1176–e1189, doi:https://doi.org/10.1002/joc.5443, URL https://rmets.onlinelibrary.wiley.com/doi/abs/10.1002/joc.5443, https://rmets.onlinelibrary.wiley.com/doi/pdf/10.1002/joc.5443.

List of Tables

Table 1. Reanalysis Product Summary Information

Reanalysis	Grid	# levels	model top height	UTLS ∼level spacing	reference(s)
MERRA-2	0.625°x0.5°	72	0.01 hPa	1.2 km	Gelaro et al. (2017)
ERA-Interim	0.75°x0.75°	60	0.1 hPa	1 km	Dee et al. (2011b)
JRA-55	0.56°x0.56°[a]	60	0.1 hPa	1 km	Kobayashi et al. (2015)
MERRA[b]	*0.667°x0.5°*	*72*	*0.01 hPa*	*1.2 km*	*Rienecker et al. (2011)*
CFSR/CFSv2[b]	*0.5°x0.5°*	*64*	*∼0.26 hPa*	*1 km*	*Saha et al. (2010, 2014)*

[a] approximately, these fields are provided on a Gaussian grid.

[b] calculations from reanalyses shown in *italics* are not illustrated in this paper.

List of Figures

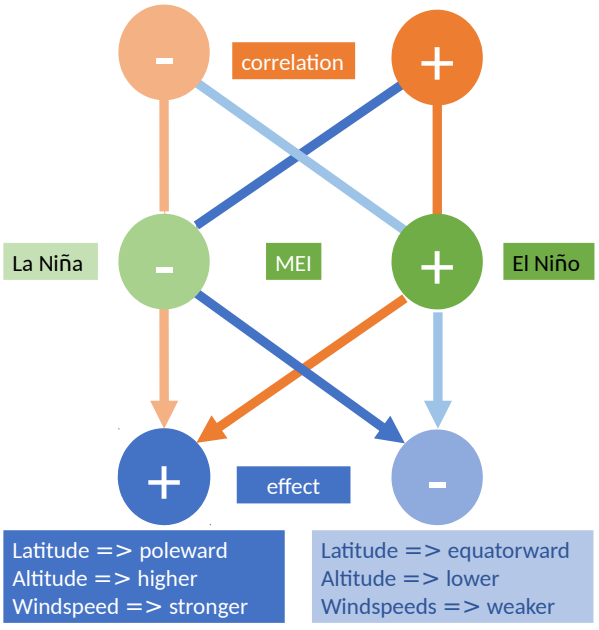

943 Figure 1. Schematic of physical changes associated with positive (follow bold arrows) and negative (follow
944 faint arrows) correlations of the upper tropospheric jet with ENSO.

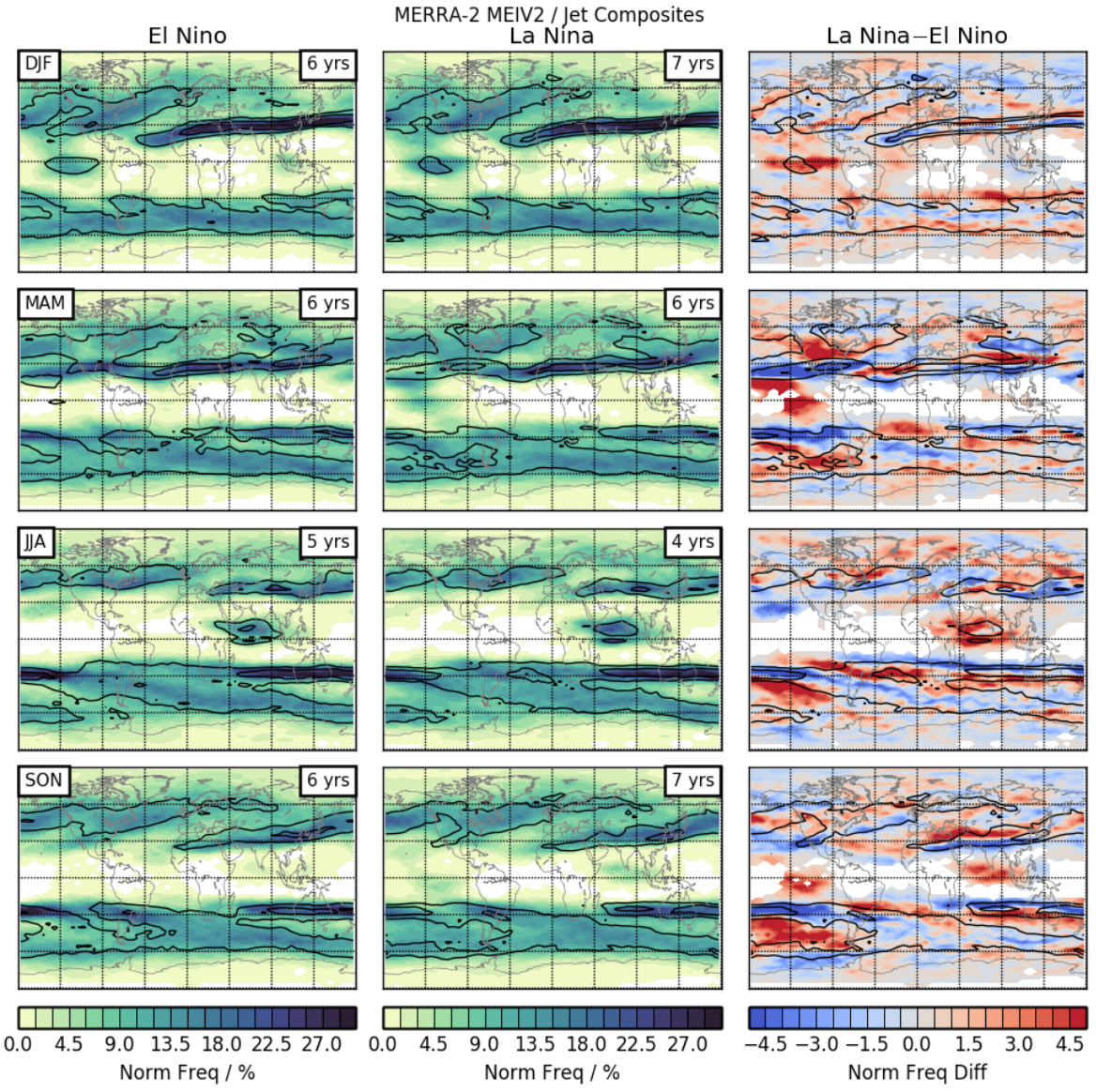

945 Figure 2. Maps of UT jet frequency distributions for El Niño (left) and La Niña (center) periods, and the
946 difference between them (right) for 1979 through 2018 (1979/80 through 2018/2019 for DJF) for (top to bot-
947 tom) DJF, MAM, JJA, and SON. from the MERRA-2 reanalysis. Frequency distributions are calculated in 6°
948 longitude by 3° latitude bins, and normalized as described in the text (Section b). 10% and 20% contours for El
949 Niño (La Niña) are overlaid on the La Niña (El Niño) panels. The ENSO threshold is MEIv2 magnitude greater
950 than 0.94.

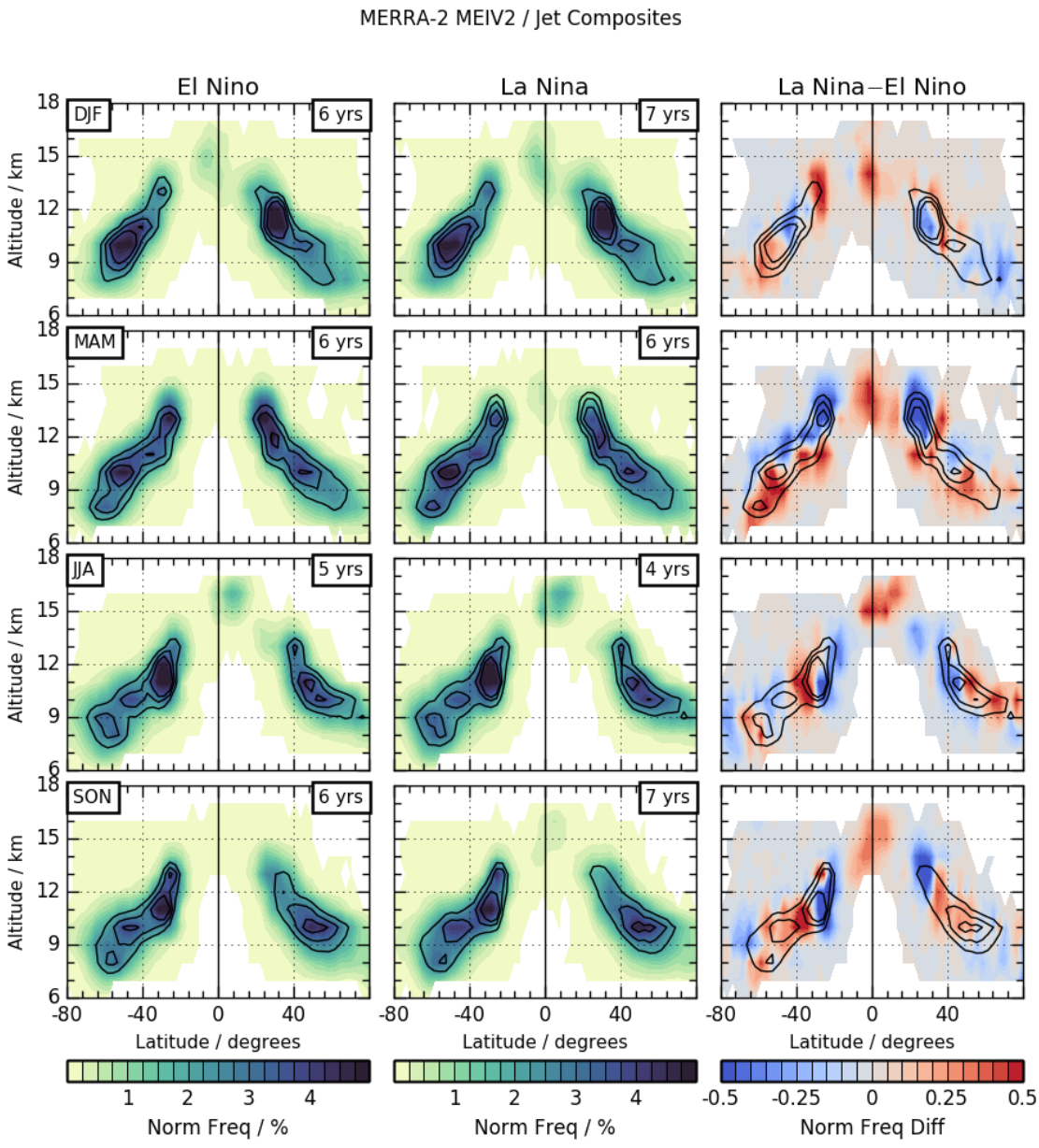

951 Figure 3. Latitude/altitude cross-sections of UT jet frequency distributions for El Niño (left) and La Niña
952 (center) periods, and the difference between them (La Niña−El Niño, right) for 1979 through 2018 (1979/80
953 through 2018/2019 for DJF) for (top to bottom) DJF, MAM, JJA, and SON. Frequency distributions are calcu-
954 lated in 3° latitude by 1 km altitude bins, and normalized as described in the text (Section b). 2%, 3%, and 4%
955 contours for El Niño (La Niña) are overlaid on the La Niña (El Niño) panels. The ENSO threshold is MEIv2
956 magnitude greater than 0.94.

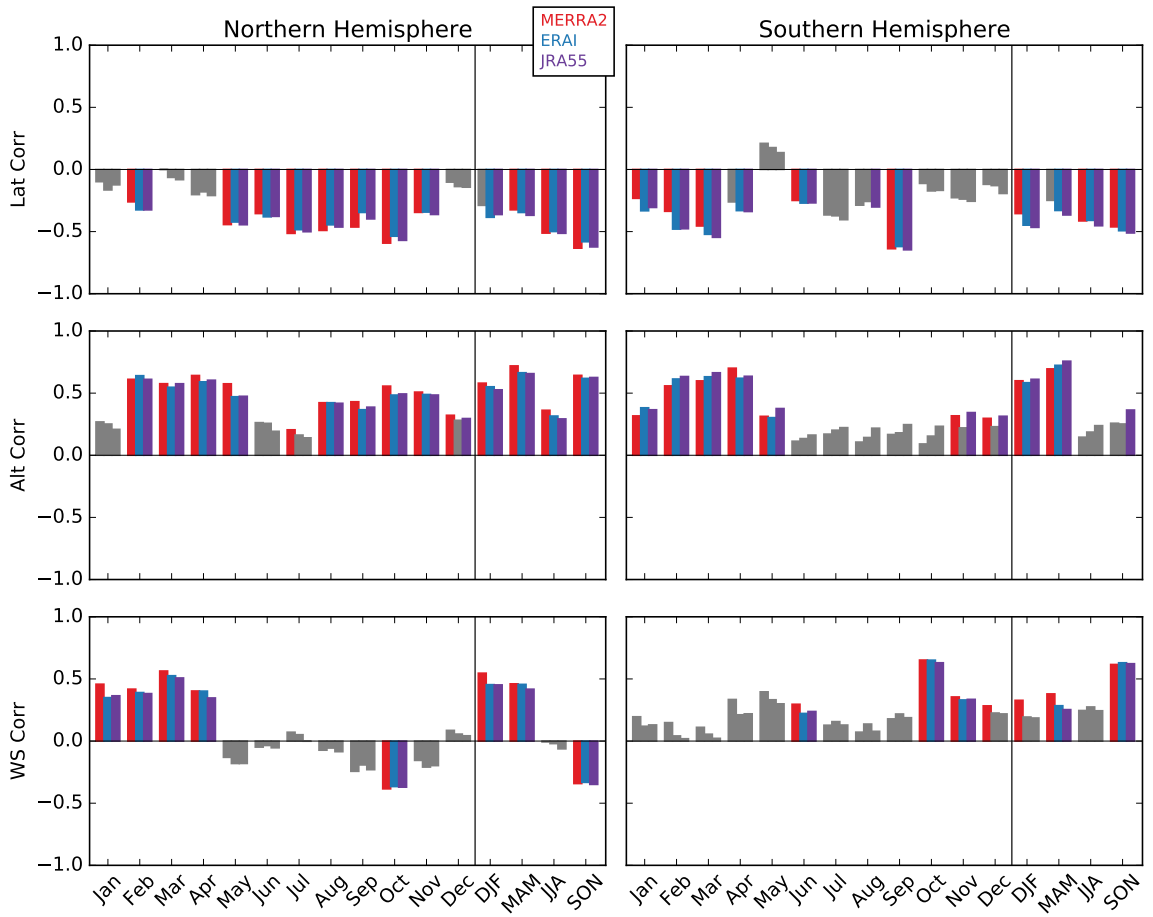

Figure 4. Correlations of monthly and seasonal 1979–2018 (1979/80 through 2018/2019 for DJF) subtropical jet latitude (top), altitude (center), and windspeed (bottom) with the MEIv2, for MERRA-2 (red, left of triplet), ERA-Interim (blue, center of triplet), and JRA-55 (purple, right of triplet). Bars show correlation coefficients and are shown in reanalysis colors when the correlations are significant at at least the 95% confidence level using a bootstrap analysis (see text, Section 2b). Absolute value of latitude is used in the SH, so positive (negative) latitude correlations always indicate that El Niño (La Niña) is associated with a more poleward jet position.

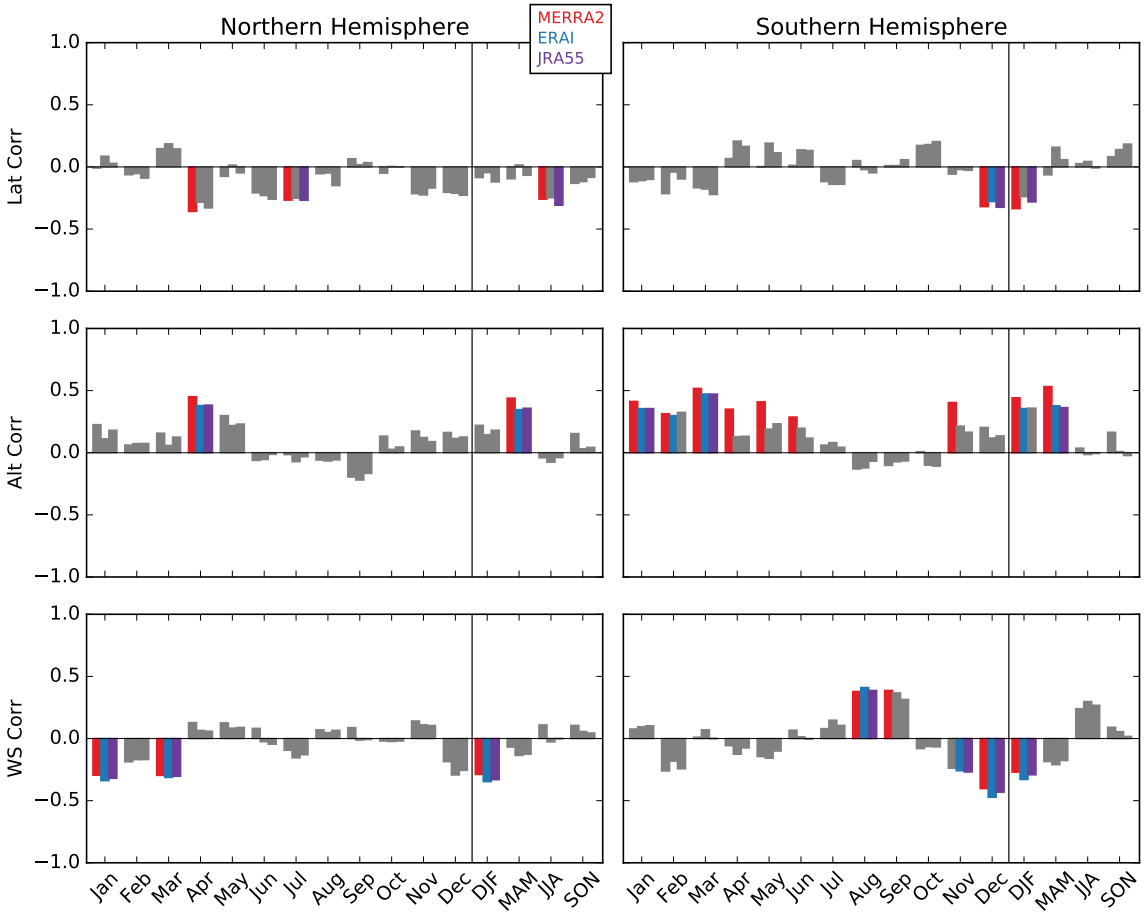

Figure 5. As in Fig. 4, but for the polar jet.

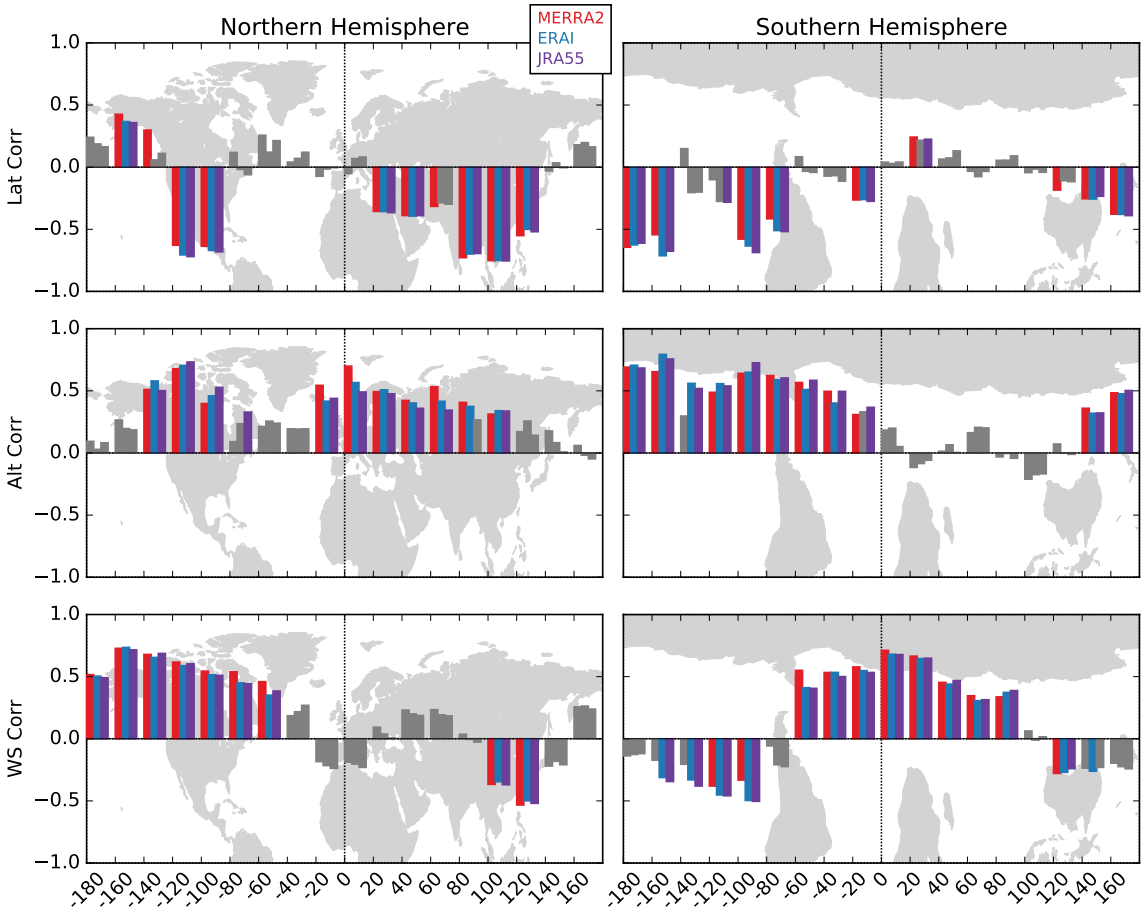

963 Figure 6. As in Fig. 4 but for correlations in 20° longitude bins for DJF. Maps are underlaid to provide
964 a geographical reference, and are inverted in the SH as a reminder that we use absolute value of latitude, so
965 poleward is always positive.

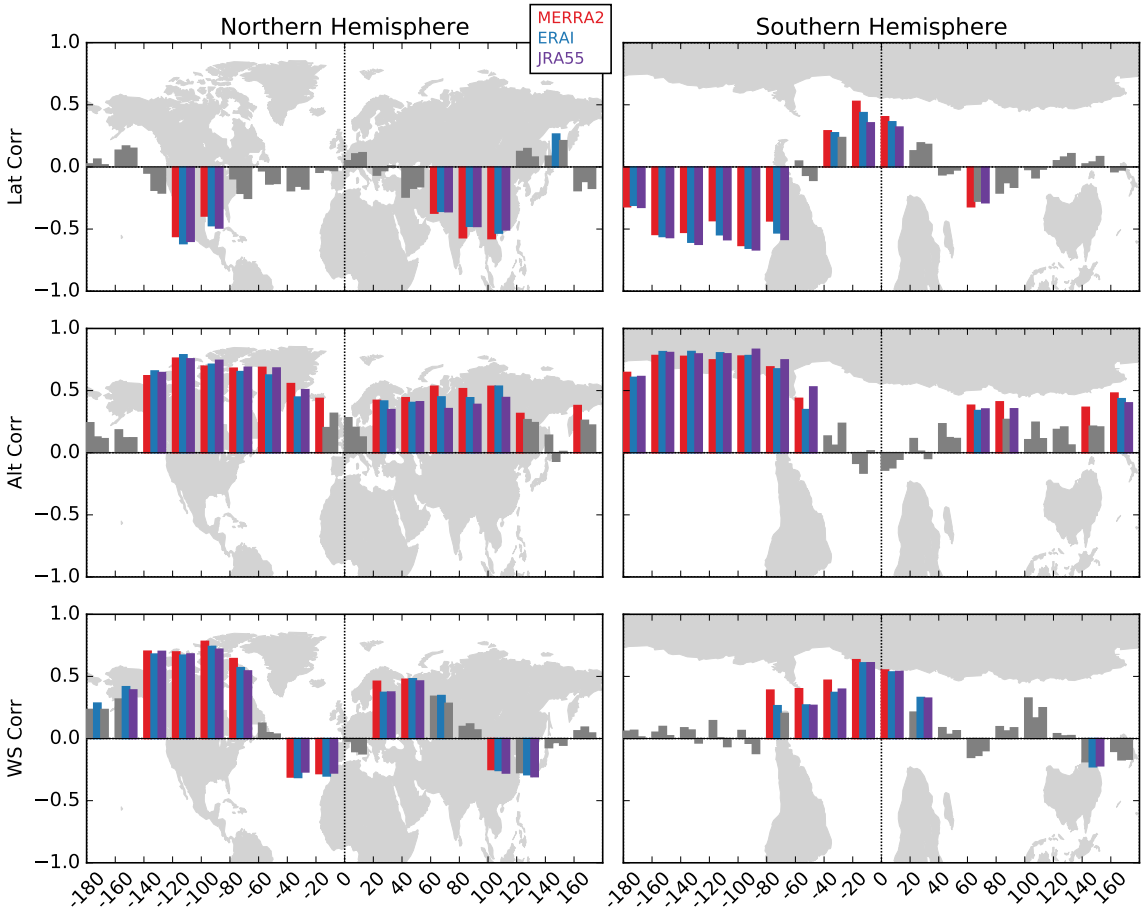

Figure 7. As in Fig. 6 but for MAM.

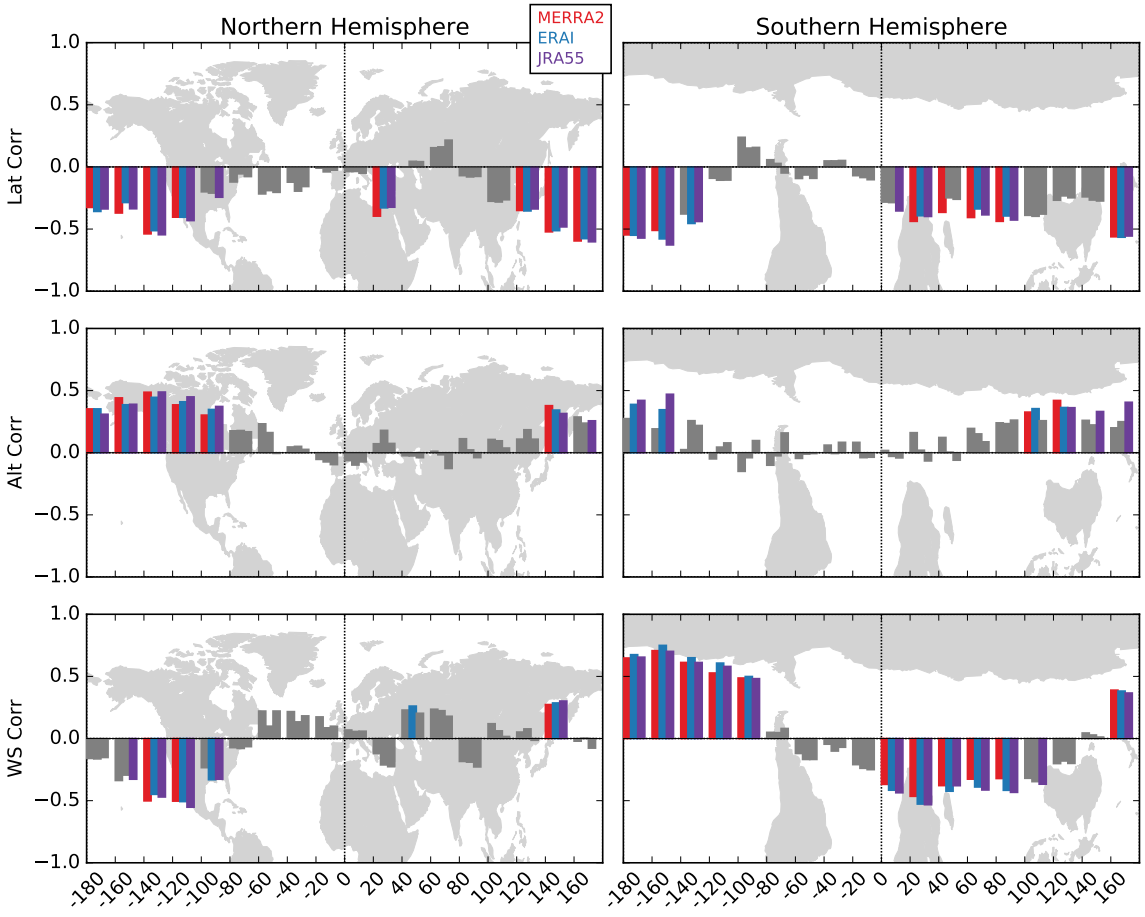

Figure 8. As in Fig. 6 but for JJA.

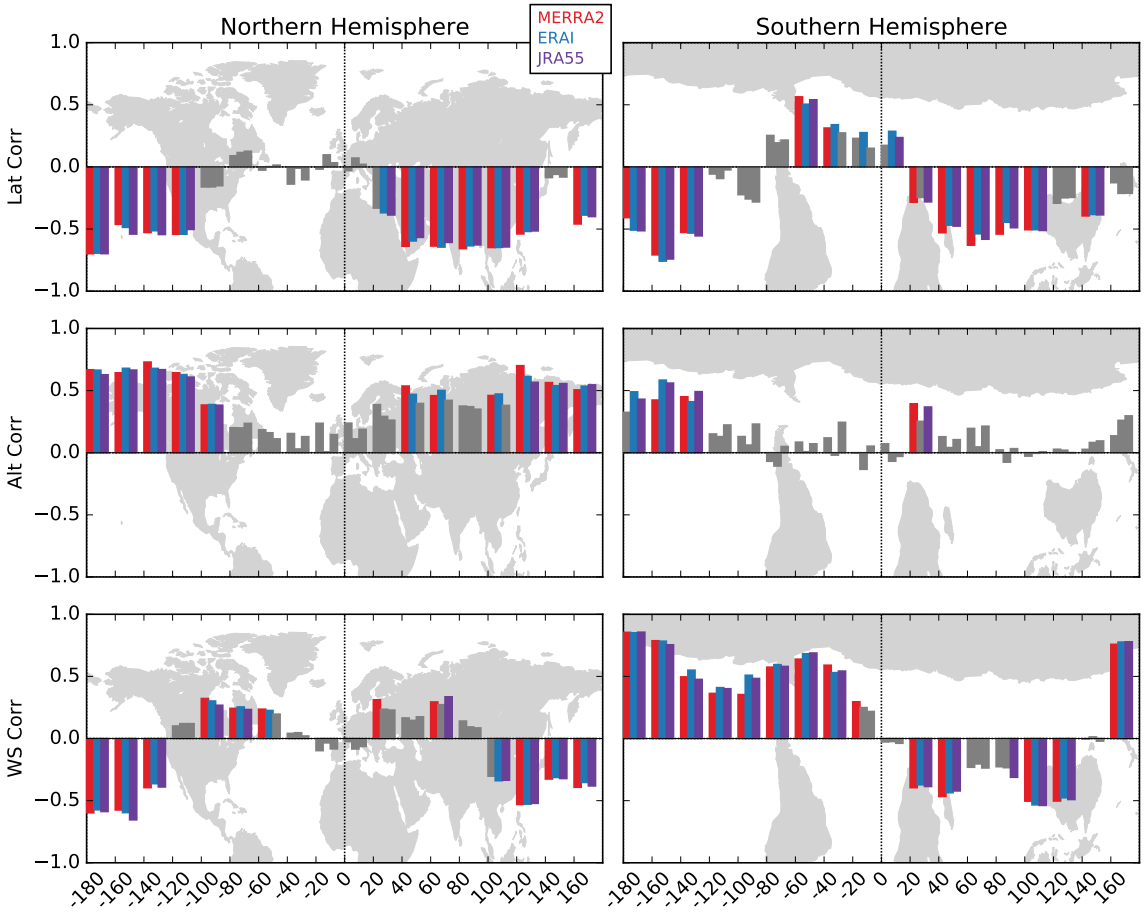

Figure 9. As in Fig. 6 but for SON.

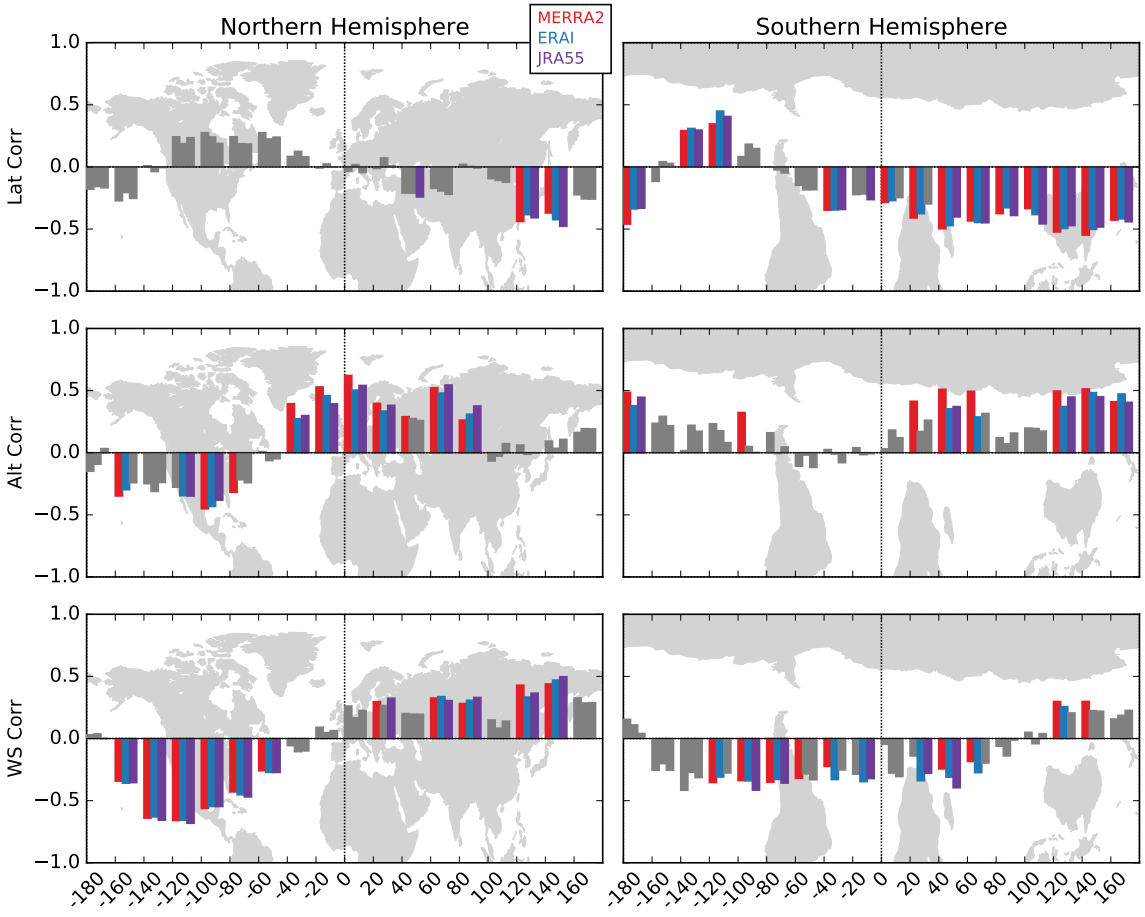

Figure 10. As in Fig. 6 but for the polar jet.

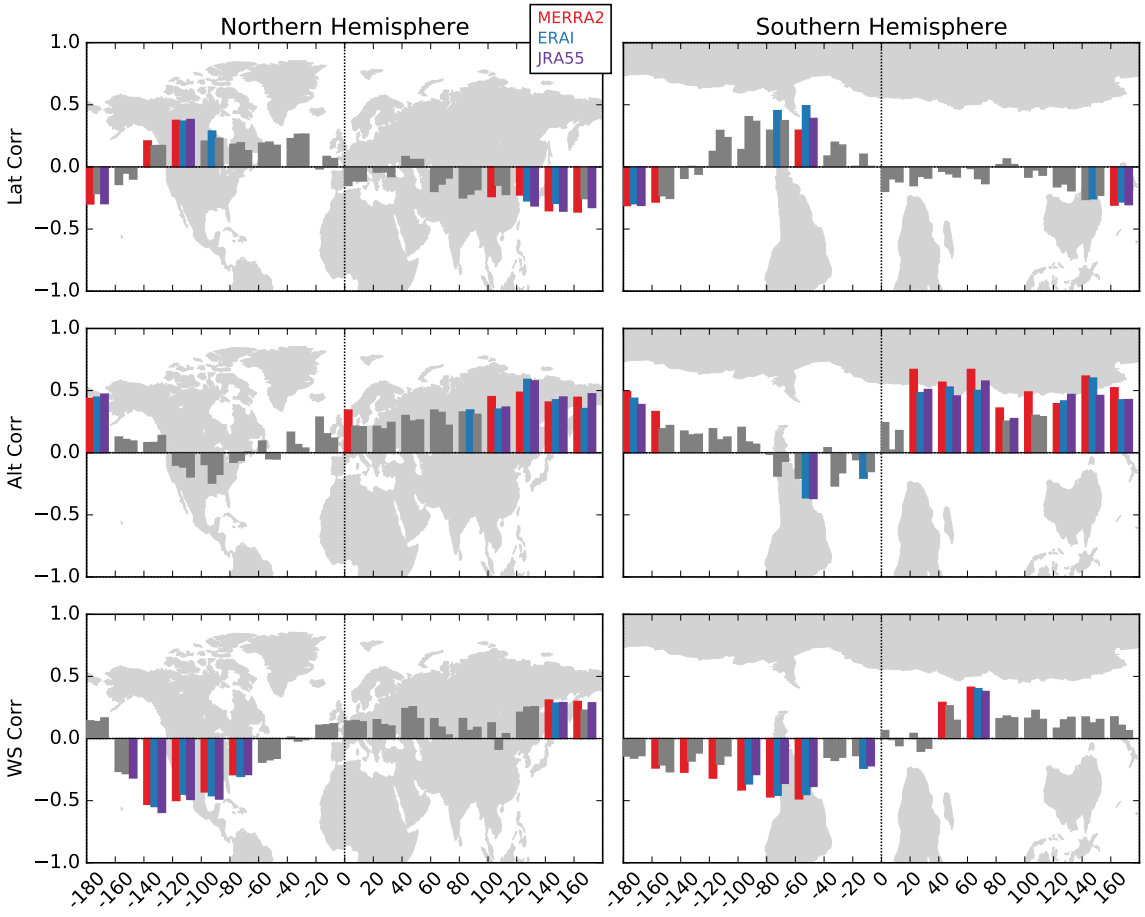

Figure 11. As in Fig. 7 but for the polar jet.

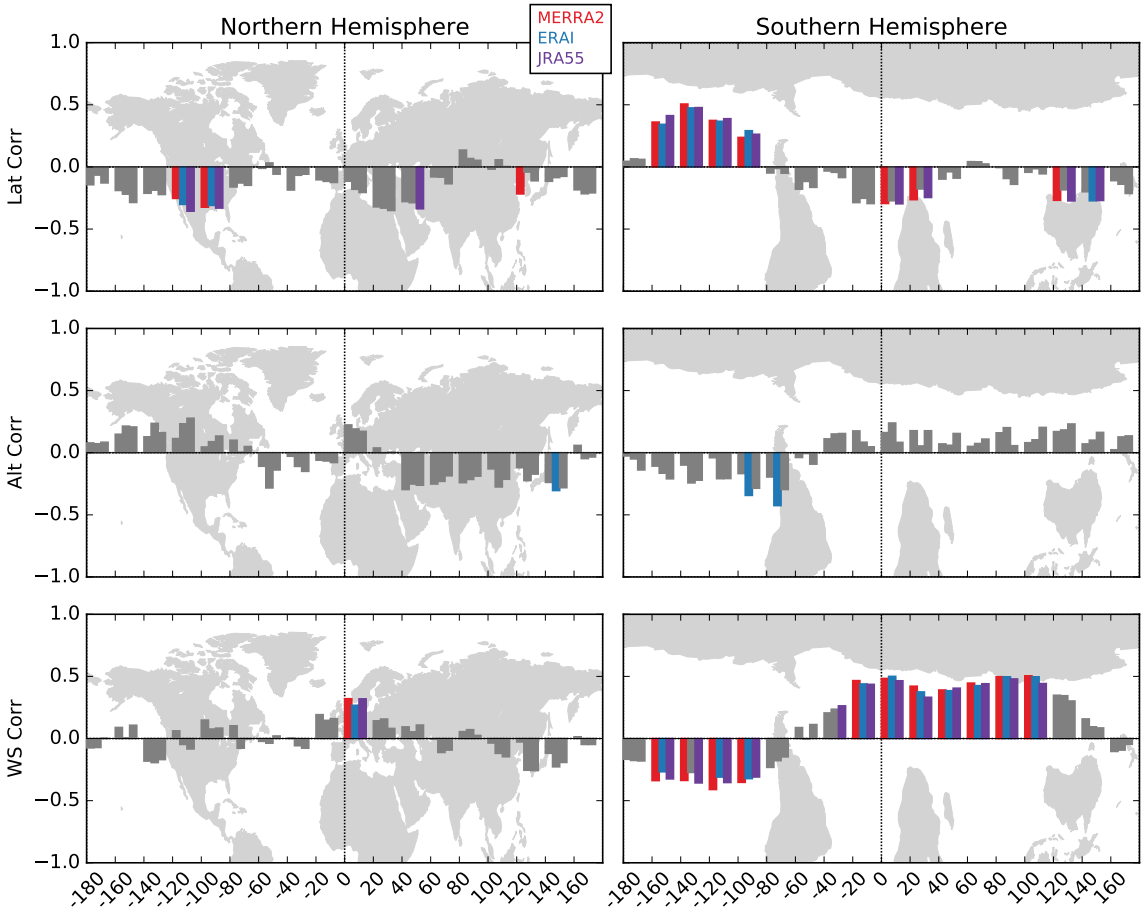

Figure 12. As in Fig. 8 but for the polar jet.

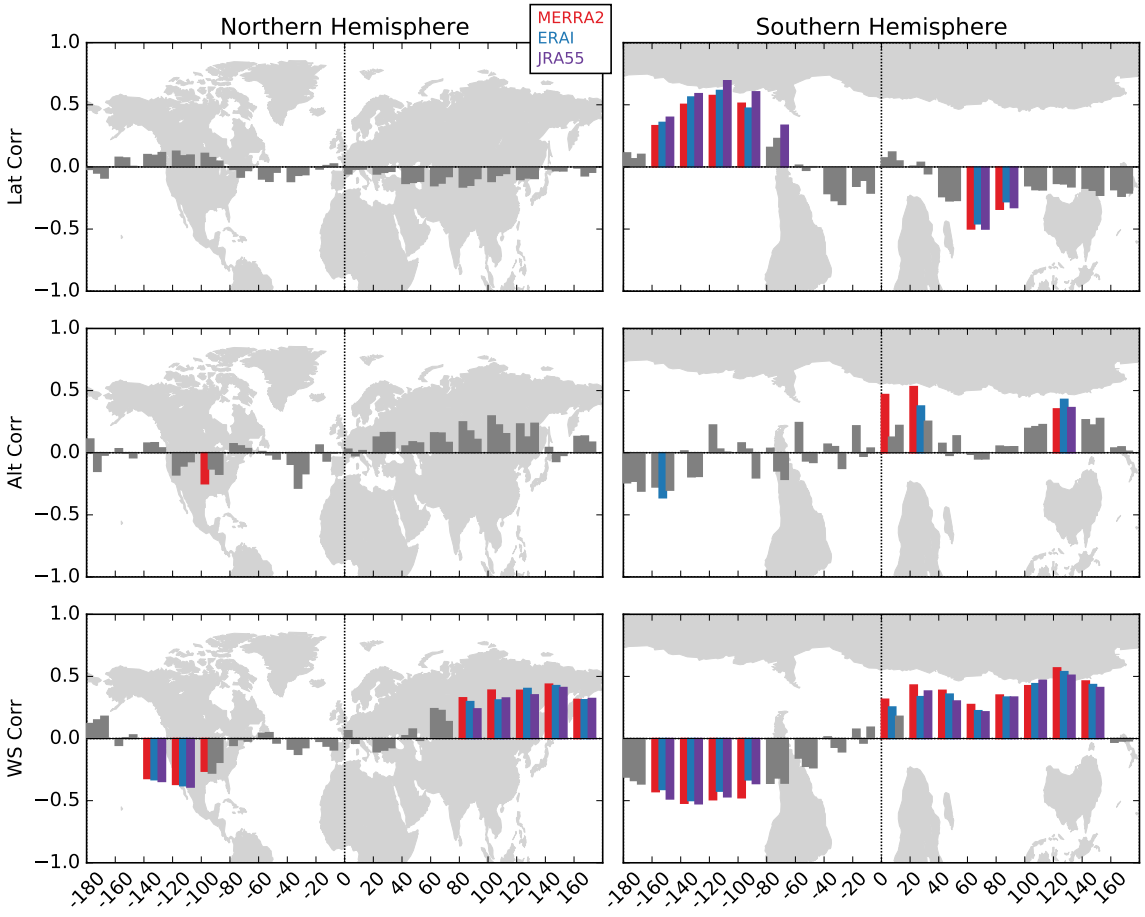

Figure 13. As in Fig. 9 but for the polar jet.

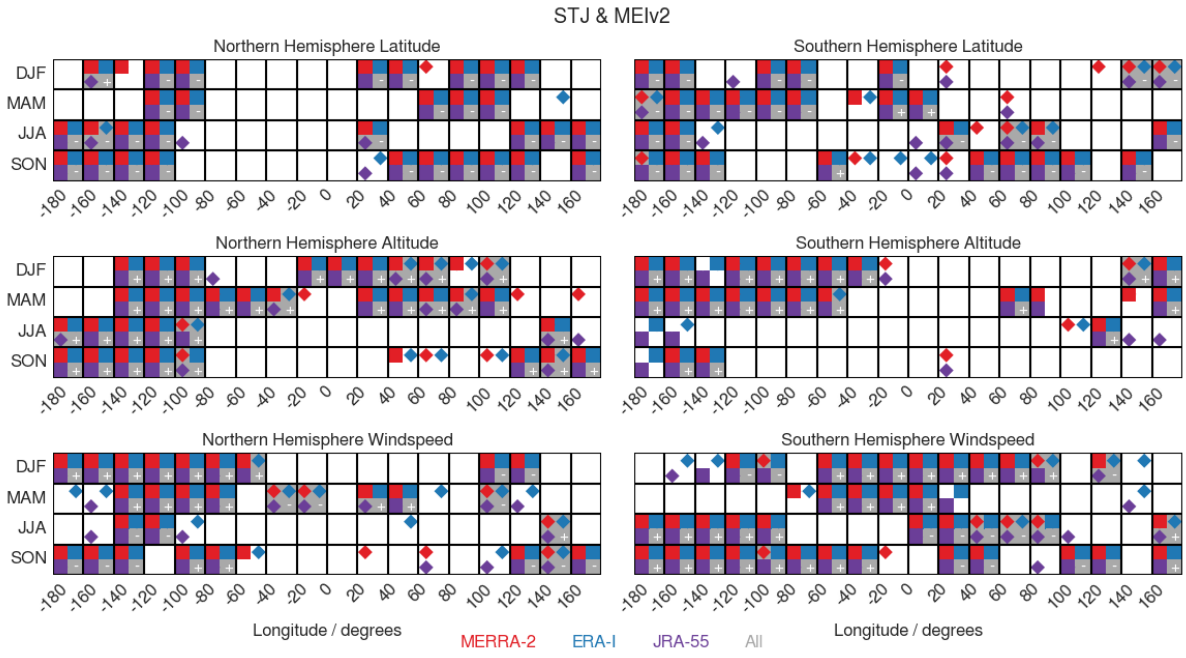

Figure 14. Summary matrix of significant STJ latitude (top), altitude (center), and windspeed (bottom) correlations with MEIv2. For each season and longitude, the top left, top right, and bottom left boxes of each season/region square are completely filled when the MERRA-2 (red), ERA-Interim (blue), and JRA-55 (purple), respectively, correlations are significant above the 99% confidence level. The same boxes are filled with diamonds when the correlations are significant between the 95% and 99% confidence levels. A grey background indicates that the correlations for all three reanalysis have the same sign and are significant at least at the 95% confidence level; the sign of the correlation in these cases is given in the lower right (grey) box.

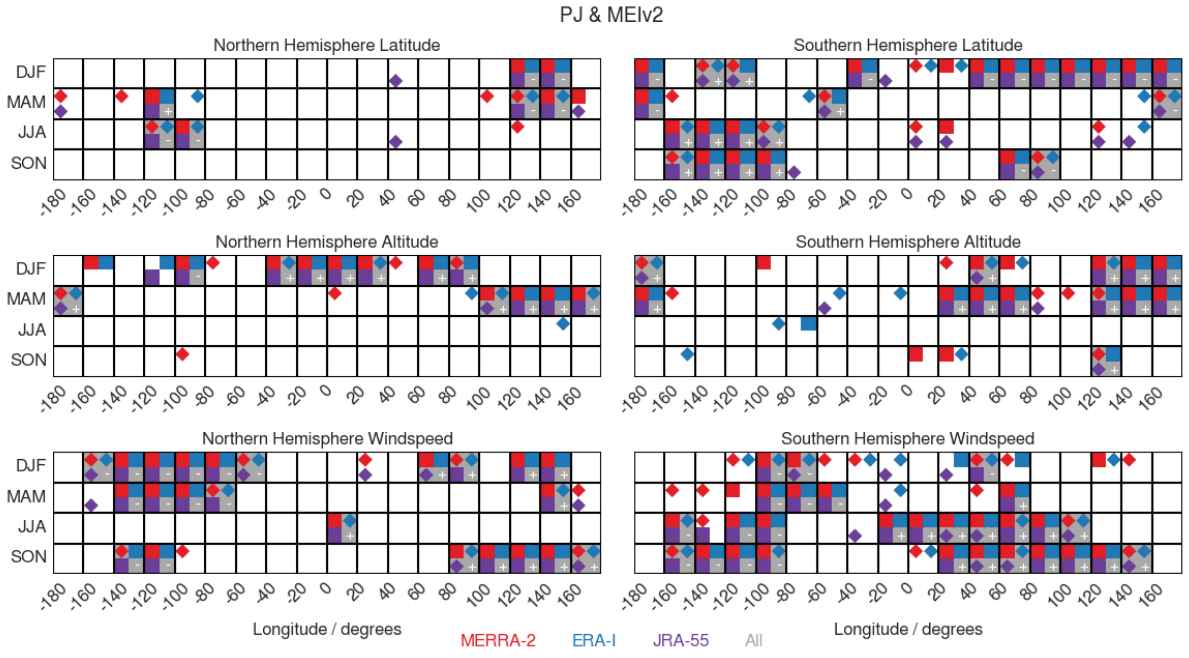

Figure 15. As in 14, but for the polar jet.